

Nonperturbative dynamics of hadronic scatterings*

Mateus Broilo da Rocha

Federal University of Rio Grande do Sul

Doctoral thesis

Adviser: Prof. Dr. Emerson Gustavo de Souza Luna

*This research was supported by CNPq grant 141496/2015-0.

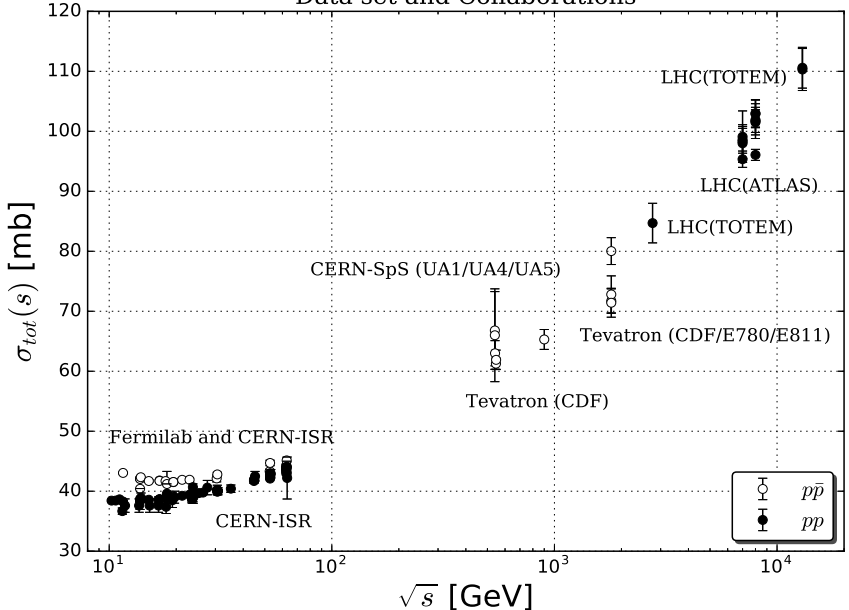
Outline

- ▶ Mini-introduction
 - Experimental data
 - Quick inspection on kinematics
 - Eikonal formalism
- ▶ Regge-Gribov based analysis
 - Regge theory
 - Phenomenology
 - Results
- ▶ QCD-inspired analysis
 - Quantum Chromodynamics
 - QIM formalism
 - Results
- ▶ Conclusions

Introduction

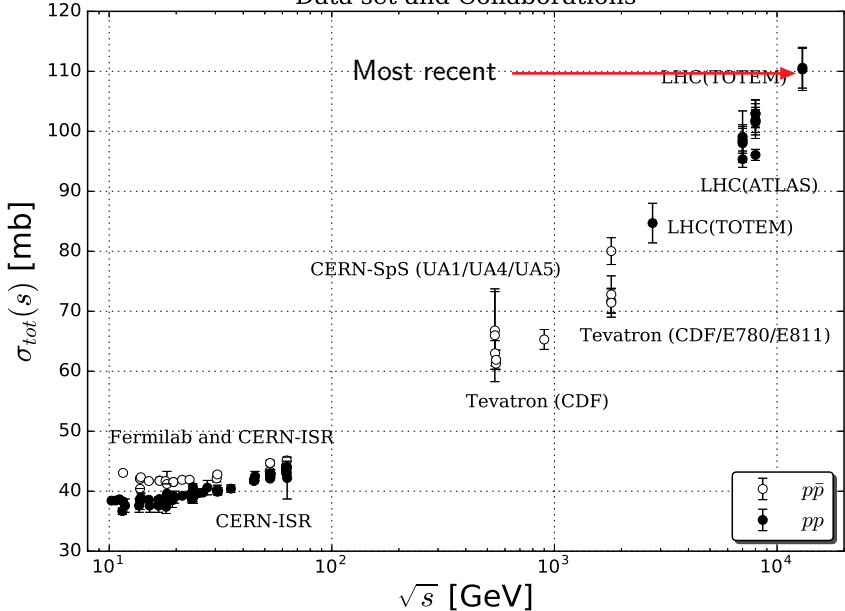
- ▶ The study of hadron-hadron total cross sections has been a subject of intense theoretical and experimental interest
- ▶ The recent measurements of pp elastic, inelastic and total cross sections at the LHC by the TOTEM Collaboration
 - ⇒ have enhanced the interest in the subject
 - ⇒ have become a pivotal source of information for selecting models and theoretical methods
- ▶ At present QCD-inspired formalism is one of the main theoretical approaches used to describe the observed increase of σ_{tot}^{hh}
- ▶ However, the recent LHC data provides a unique constraint on the soft Pomeron parameters

Data set and Collaborations



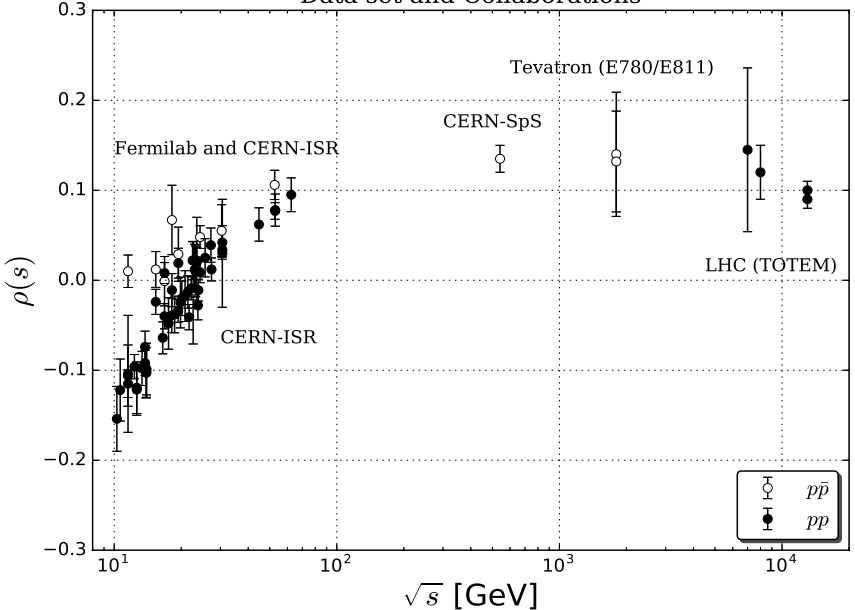
Total cross section data for pp and $p\bar{p}$ scattering.

Data set and Collaborations



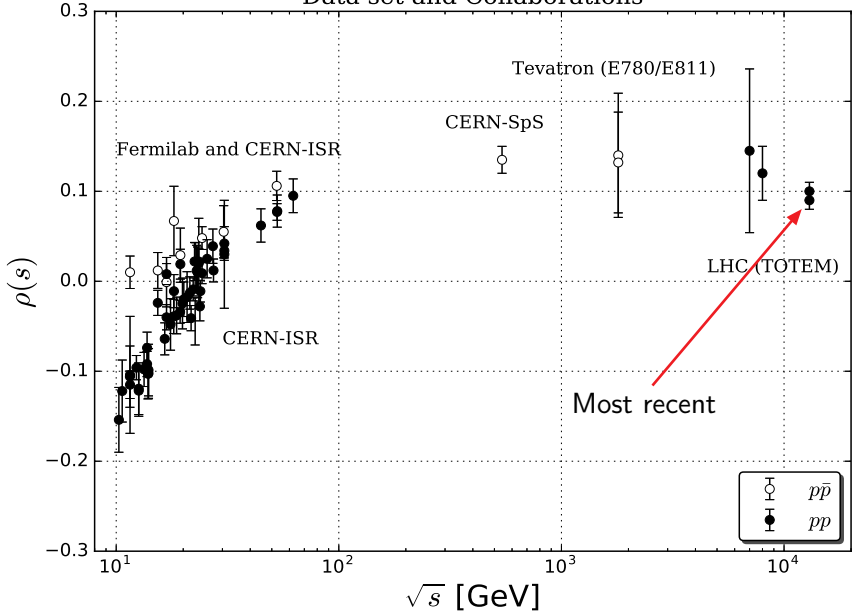
Total cross section data for pp and $p\bar{p}$ scattering.

Data set and Collaborations



Ratio of the real to imaginary part of the forward scattering amplitude.

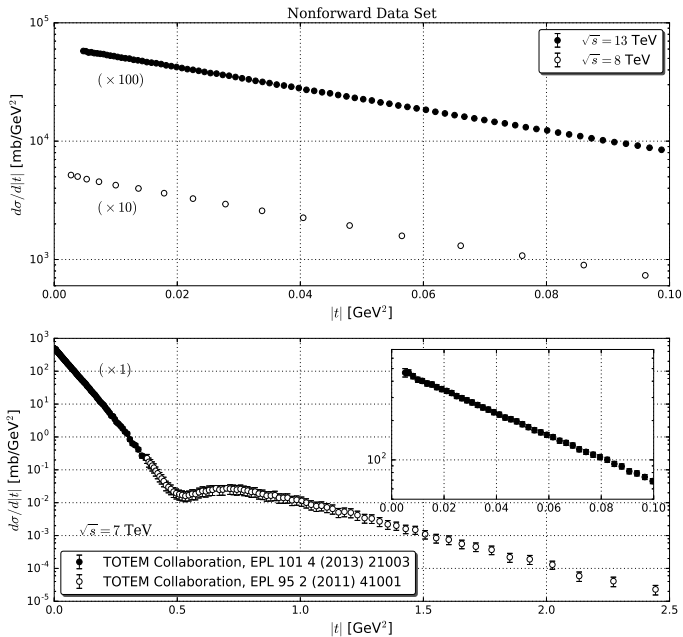
Data set and Collaborations



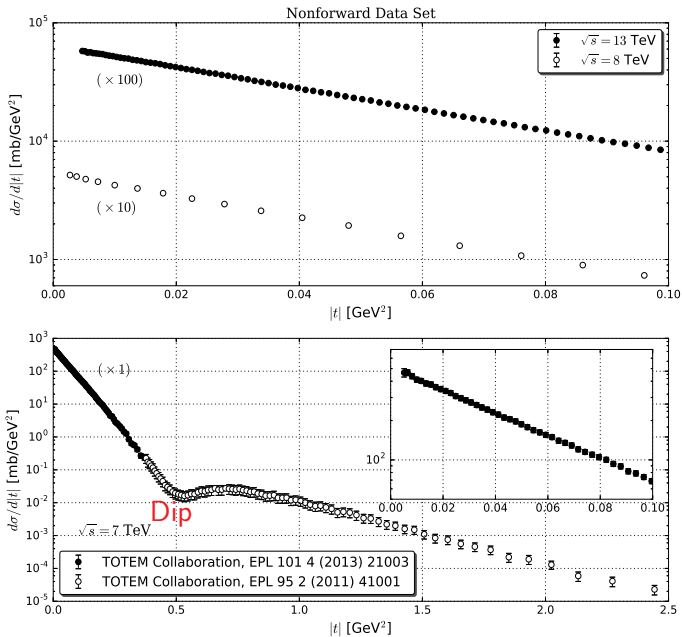
Ratio of the real to imaginary part of the forward scattering amplitude.

Experimental high-energy data

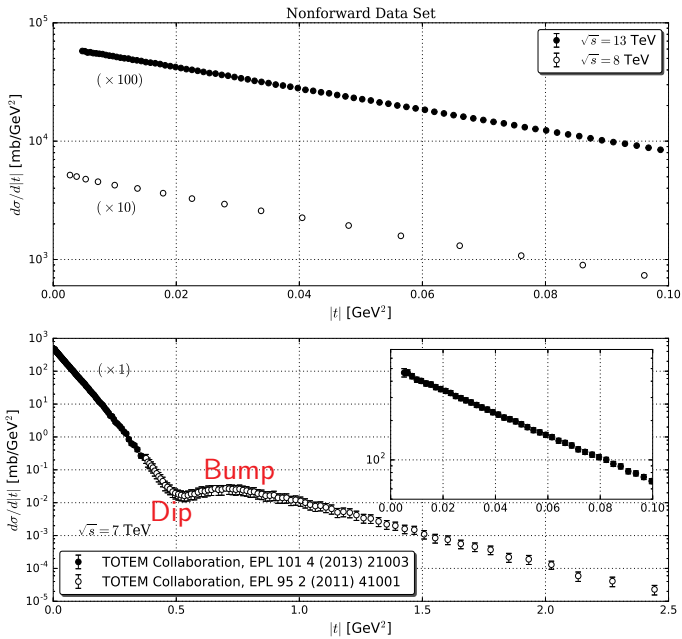
Collaboration	Reference	\sqrt{s} (TeV)	σ_{tot} (mb)
TOTEM	CERN-EP-2017-321	2.76	84.7 ± 3.3
	EPL96 (2011) 21002	7	98.3 ± 2.8
	EPL101 (2013) 21003	7	98.6 ± 2.2
	EPL101 (2013) 21004	7	98.0 ± 2.5
	EPL101 (2013) 21004	7	99.1 ± 4.3
	PRL111 (2013) 012001	8	101.7 ± 2.9
	NPB 899 (2015) 527	8	101.5 ± 2.1
	NPB 899 (2015) 527	8	101.9 ± 2.1
	EPJ C76 (2016) 661	8	102.9 ± 2.3
	EPJ C76 (2016) 661	8	103.0 ± 2.3
	CERN-EP-2017-321	13	110.6 ± 3.4
	CERN-EP-2017-335	13	110.3 ± 3.5
ATLAS	NPB 899 (2014) 486	7	95.4 ± 1.4
	PLB 761 (2016) 158	8	96.07 ± 0.92
Collaboration	Reference	\sqrt{s} (TeV)	ρ
TOTEM	EPL101 (2013) 21004	7	0.145 ± 0.091
	EPJ C76 (2016) 661	8	0.120 ± 0.030
	CERN-EP-2017-335	13	0.090 ± 0.010
	CERN-EP-2017-335	13	0.100 ± 0.010



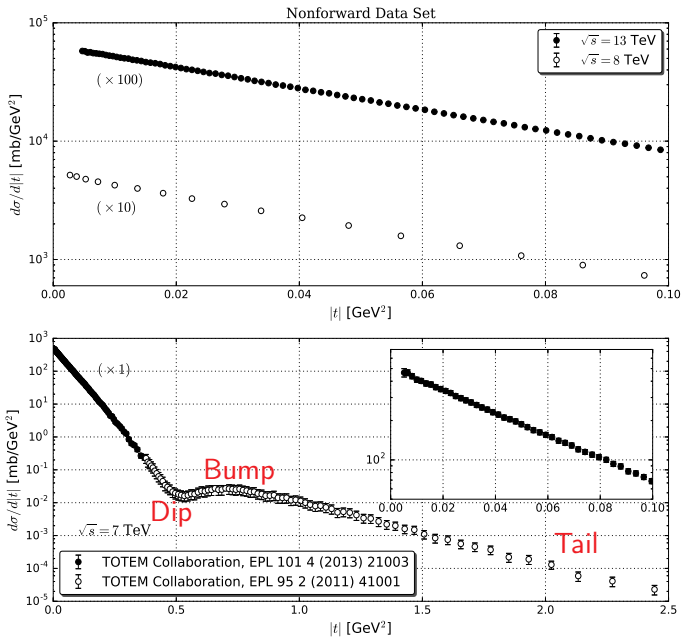
Elastic $p p$ differential cross section.



Elastic pp differential cross section.



Elastic pp differential cross section.



Elastic pp differential cross section.

Quick inspection on kinematics

- ▶ Collisions lead to scatterings

$$1 + 2 \rightarrow 3 + 4 + 5 + \dots$$

- ▶ Two-body exclusive process

$$1 + 2 \rightarrow 3 + 4 \text{ (s-channel)}$$

- ▶ Mandelstam invariants

$$s = (P_1 + P_2)^2 = (P_3 + P_4)^2$$

$$t = (P_1 - P_3)^2 = (P_2 - P_4)^2$$

$$u = (P_1 - P_4)^2 = (P_2 - P_3)^2$$

constrained to

$$s + t + u = \sum_{i=1}^4 m_i^2$$

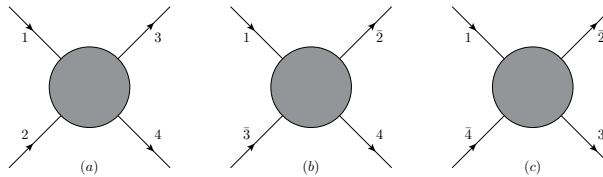
Quick inspection on kinematics

- ▶ In the crossed channel (time-reversed)

$$1 + \bar{3} \rightarrow \bar{2} + 4 \text{ (t-channel)}$$

- ▶ By crossing-symmetry

$$F_{1+2 \rightarrow 3+4}(s, t, u) = F_{1+\bar{3} \rightarrow \bar{2}+4}(t, s, u)$$



Quick inspection on kinematics

- ▶ Elastic scattering: the incident particles corresponds exactly to those ones in the final state.

$$1 + 2 \rightarrow 1' + 2'$$

- ▶ Simplest kinematic processes → theoretical description is extremely difficult.
- ▶ Elastic $p p$ and $\bar{p} p$ scattering

$$s\text{-channel} : p + p \rightarrow p + p$$

$$t\text{-channel} : \bar{p} + p \rightarrow \bar{p} + p$$

Eikonal formalism

- ▶ Partial wave approximation

$$f(\mathbf{k}, \mathbf{k}') = f(k, \theta) = \sum_{\ell=0}^{\infty} (2\ell + 1) a_\ell(k) P_\ell(\cos \theta)$$

- ▶ By taking the high-energy limit

$$f(s, t) = ik \int_0^{\infty} db b J_0(b\sqrt{-t}) \underbrace{\left[1 - e^{i\chi(s, b)} \right]}_{\equiv \Gamma(s, b)}$$

- ▶ Unitarity condition

$$\Gamma(s, b) = \operatorname{Re} \Gamma(s, b) + i \operatorname{Im} \Gamma(s, b)$$

$$2\operatorname{Re} \Gamma(s, b) = |\Gamma(s, b)|^2 + (1 - e^{-2\chi_I})$$

Eikonal formalism

- ▶ Total cross section

$$\begin{aligned}\sigma_{tot}(s) &= 2\pi \int_0^\infty db b 2 \operatorname{Re} \Gamma(s, b) \\ &= 4\pi \int_0^\infty db b [1 - e^{-\chi_I} \cos \chi_R] = \sigma_{el} + \sigma_{in}\end{aligned}$$

- ▶ Elastic differential cross section

$$\frac{d\sigma}{dt}(s, t) = \pi \left| i \int_0^\infty db b J_0(b\sqrt{-t}) [1 - e^{i\chi(s, b)}] \right|^2$$

- ▶ ρ -parameter

$$\rho(s) = \frac{\operatorname{Re} \left\{ i \int_0^\infty db b [1 - e^{i\chi(s, b)}] \right\}}{\operatorname{Im} \left\{ i \int_0^\infty db b [1 - e^{i\chi(s, b)}] \right\}} = \frac{\int_0^\infty db b e^{-\chi_I} \sin \chi_R}{\int_0^\infty db b (1 - e^{-\chi_I} \cos \chi_R)}$$

Regge theory

Regge theory: Basics

- ▶ The Regge pole idea → strong interaction is described by the exchange of Regge trajectories
- ▶ Each pole corresponds to singularities in the partial wave amplitude

$$\ell = \alpha(t)$$

- $\alpha(t)$ stands for the Regge trajectory
- ▶ At high-energy
 - ▶ Asymptotically the Pomeron dominates at high energies, whereas the secondary Reggeons are responsible for the low-energy region
 - ▶ Fundamental result:

$$A(s, t) \underset{s \rightarrow \infty}{\sim} s^{\alpha(t)}$$

Regge theory: Basics

- ▶ The Regge pole idea → strong interaction is described by the exchange of Regge trajectories
- ▶ Each pole corresponds to singularities in the partial wave amplitude

$$\ell = \alpha(t)$$

- $\alpha(t)$ stands for the Regge trajectory
- ▶ At high-energy

$$A(s, t) \underset{s \rightarrow \infty}{\sim} s^{\alpha(t)}$$

- ▶ Asymptotically the **Pomeron** dominates at **high energies**, whereas the **secondary Reggeons** are responsible for the **low-energy region**
- ▶ **Fundamental result:** the leading complex angular momentum singularity of the partial wave amplitude in a given channel, determines the **asymptotic behavior** of the scattering amplitude in the crossed channel

Regge theory: Basics

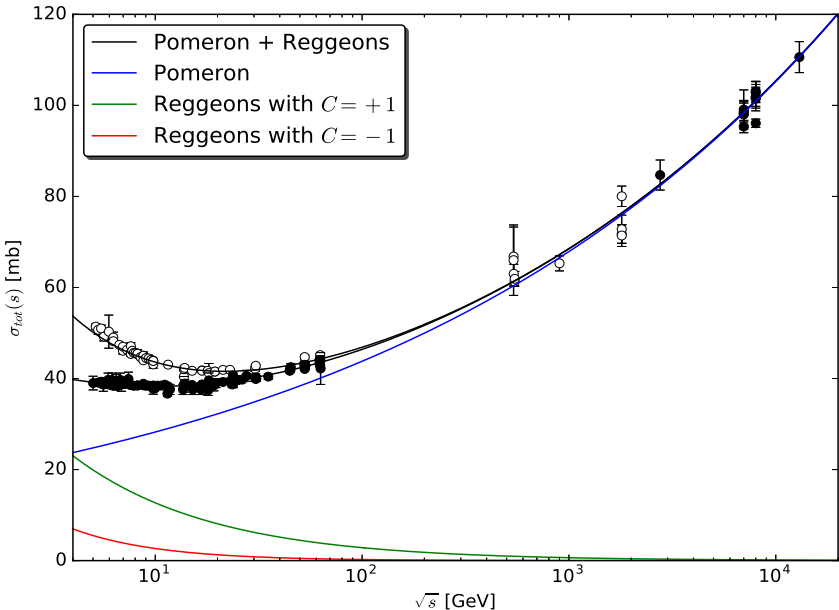
- ▶ The Regge pole idea → strong interaction is described by the exchange of Regge trajectories
- ▶ Each pole corresponds to singularities in the partial wave amplitude

$$\ell = \alpha(t)$$

- $\alpha(t)$ stands for the Regge trajectory
- ▶ At high-energy

$$A(s, t) \underset{s \rightarrow \infty}{\sim} s^{\alpha(t)}$$

- ▶ Asymptotically the Pomeron dominates at high energies, whereas the secondary Reggeons are responsible for the low-energy region
- ▶ Fundamental result: the ~~leading complex angular momentum singularity~~ **Regge pole** of the partial wave amplitude in a given channel, determines the asymptotic behavior of the scattering amplitude in the crossed channel



Simple Regge based analysis. Contribution from each Reggeon amplitude at the Born-level, respectively.

Regge theory: Regge poles → Long story short

- ▶ The scattering amplitude is written as the **Watson-Sommerfeld transform** of the **partial wave series**
 - The dominant contribution in the case of ***t*-channel** exchange

$$A(s, t) \underset{s \rightarrow \infty}{\simeq} \sum_{\xi=\pm 1} \sum_{i_\xi} -\gamma_{i_\xi}(t) \frac{1 + \xi e^{-i\pi\alpha_{i_\xi}(t)}}{\sin \pi\alpha_{i_\xi}(t)} s^{\alpha_{i_\xi}(t)}$$

- α_{i_ξ} defines the location of the *i*-th pole → each Reggeon contribution
- $\gamma_{i_\xi}(t)$ stands for the residue function and *phenomenologically* is related to the hadron-Reggeon vertex coupling
- ▶ Leading pole → **Pomeron** $\xi = +1$

$$A(s, t) \underset{s \rightarrow \infty}{\sim} -\gamma_i(t) \frac{1 + \xi e^{-i\pi\alpha(t)}}{\sin \pi\alpha(t)} s^{\alpha(t)}$$

- ▶ New quantum number, the signature $\xi = \pm 1$
 - Then $A_\ell(t)$ can be **analytically continued** to complex ℓ -values by means of the **Watson-Sommerfeld transform**

Phenomenology

- ▶ Returning to the task in hand (description of $p\bar{p}$ and $\bar{p}p$ scatterings)...
But beforehand:
 - diffractive processes are described by **Regge theory**
 - **high-energy behavior** of the scattering amplitude → described by **singularities of the amplitude** in the **complex angular momentum plane**
- ▶ As it was previously mentioned

$$A(s, t) \propto s^{\alpha(t)}$$

- ▶ If more than one pole contributes

$$A(s, t) = \sum_i \gamma_i(t) \eta_i(t) s^{\alpha_i(t)}$$

- where $\eta_i(t) = -\frac{1+\xi e^{-i\pi\alpha_i(t)}}{\sin(\pi\alpha_i(t))}$ is the signature factor
- ▶ Straightforward

Phenomenology

- ▶ Returning to the task in hand (description of $p\bar{p}$ and $\bar{p}p$ scatterings)...
But beforehand:
 - diffractive processes are described by Regge theory
 - high-energy behavior of the scattering amplitude → described by singularities of the amplitude in the complex angular momentum plane
- ▶ As it was previously mentioned

$$A(s, t) \propto s^{\alpha(t)}$$

- ▶ If more than one pole contributes

$$A(s, t) = \sum_i \gamma_i(t) \eta_i(t) s^{\alpha_i(t)} \quad (\text{as it was also mentioned})$$

- where $\eta_i(t) = -\frac{1+\xi e^{-i\pi\alpha_i(t)}}{\sin(\pi\alpha_i(t))}$ is the signature factor
- ▶ Straightforward

Phenomenology

- ▶ Returning to the task in hand ([description of \$p\bar{p}\$ and \$\bar{p}p\$ scatterings](#))...
- But beforehand:
 - diffractive processes are described by [Regge theory](#)
 - [high-energy behavior](#) of the scattering amplitude → described by [singularities of the amplitude](#) in the [complex angular momentum plane](#)
- ▶ As it was previously mentioned

$$A(s, t) \propto s^{\alpha(t)}$$

- ▶ If more than one pole contributes

$$A(s, t) = \sum_i \gamma_i(t) \eta_i(t) s^{\alpha_i(t)} \quad (\text{as it was also mentioned})$$

- where $\eta_i(t) = -\frac{1+\xi e^{-i\pi\alpha_i(t)}}{\sin(\pi\alpha_i(t))}$ is the signature factor
- ▶ Straightforward

$$\eta(t) = -\underbrace{\frac{e^{-i\pi\alpha_i(t)/2}}{\sin\left(\frac{\pi}{2}\alpha_i(t)\right)}}_{\xi=+1}$$

Phenomenology

- ▶ Returning to the task in hand (**description of $p\bar{p}$ and $\bar{p}p$ scatterings**)...

But beforehand:

 - diffractive processes are described by **Regge theory**
 - **high-energy behavior** of the scattering amplitude → described by **singularities of the amplitude** in the **complex angular momentum plane**
- ▶ As it was previously mentioned

$$A(s, t) \propto s^{\alpha(t)}$$

- ▶ If more than one pole contributes

$$A(s, t) = \sum_i \gamma_i(t) \eta_i(t) s^{\alpha_i(t)} \quad (\text{as it was also mentioned})$$

– where $\eta_i(t) = -\frac{1+\xi e^{-i\pi\alpha_i(t)}}{\sin(\pi\alpha_i(t))}$ is the signature factor

- ▶ Straightforward

$$\eta(t) = -\underbrace{\frac{e^{-i\pi\alpha_i(t)/2}}{\sin\left(\frac{\pi}{2}\alpha_i(t)\right)}}_{\xi=+1} \quad \text{and} \quad \eta(t) = -i\underbrace{\frac{e^{-i\pi\alpha_i(t)/2}}{\cos\left(\frac{\pi}{2}\alpha_i(t)\right)}}_{\xi=-1}$$

Motivation and the forward LHC13 data

- ▶ New experimental information on σ_{tot} and ρ at $\sqrt{s} = 13$ TeV were reported by the TOTEM Collaboration

$$\sigma_{tot}^{pp} = 110.6 \pm 3.4 \text{ mb}$$

$$\rho^{pp} = 0.10 \pm 0.01 \text{ and } 0.09 \pm 0.01$$

- ▶ the rising of σ_{tot} is in agreement with the trend of previous measurements at 7 and 8 TeV
- ▶ unexpected decrease in the value of the ρ^{pp}
 - Some possible hint from an **Odderon contribution?**
- ▶ analyses have favored the **Pomeron** dominance, at least, up to 8 TeV
 - develop detailed tests on the applicability of the **Pomeron models**
- ▶ Indeed, and **odd-under-crossing** asymptotic contribution provides quite good descriptions of the experimental data

Recently: Thu, 9 Nov 2017 08h13min13s

Did TOTEM experiment discover the Odderon?

Evgenij Martynov^a, Basarab Nicolescu^b

^a*Bogolyubov Institute for Theoretical Physics, Metrologichna 14b, Kiev, 03680 Ukraine*

^b*Faculty of European Studies, Babes-Bolyai University, Emmanuel de Martonne Street 1, 400090 Cluj-Napoca, Romania*

Abstract

The present study shows that, beyond any doubt, the new TOTEM datum $\rho^{pp} = 0.098 \pm 0.01$ can be considered as the first experimental discovery of the Odderon, namely in its maximal form.

Keywords: Froissaron, Maximal Odderon, total cross sections, the phase of the forward amplitude.

Odderon.

Where does it come from?

What does it eat?

- ▶ So far: Hypothetical Regge trajectory
- ▶ May play some rôle in high-energy scattering
- ▶ Conceived as the $C = P = -1$ partner of the Pomeron
- ▶ Defined as a j -plane singularity of the crossing-odd amplitude, \mathcal{A}_- , near $j = 1$ at $t = 0$.
- ▶ Its existence, **FOR WHICH THERE IS PRESENTLY NO CONCLUSIVE EVIDENCE FROM THE DATA**, at least at low- t , would entail differences between:
 - the asymptotic scattering amplitudes
 - the cross-section of pp and $\bar{p}p$

Soft pomeron models: General analytic parametrization

- ▶ In the Regge-Gribov formalism:

$$\sigma_{tot}(s) \propto s^{\alpha_0 - 1} \ln^{N-1} s$$

simple pole ($N = 1$) $\Rightarrow \sigma \propto s^{\alpha_0 - 1}$;

double pole ($N = 2$) at $\alpha_0 = 1 \Rightarrow \sigma \propto \ln(s)$;

triple pole ($N = 3$) at $\alpha_0 = 1 \Rightarrow \sigma \propto \ln^2(s)$.

- ▶ Sum of contributions associated with Reggeons R and Pomerons P

$$\sigma_{tot}(s) = \sigma^R(s) + \sigma^P(s)$$

- ▶ nondegenerated even and odd Regge trajectories

$$\sigma^R(s) = a_1 \left[\frac{s}{s_0} \right]^{-b_1} + \tau a_2 \left[\frac{s}{s_0} \right]^{-b_2}$$

- ▶ For the Pomeron contributions (even under crossing)

$$\sigma^P(s) = A + B \left[\frac{s}{s_0} \right]^{\epsilon} + C \ln \left(\frac{s}{s_0} \right) + D \ln^2 \left(\frac{s}{s_0} \right)$$

General analytic parametrization

- ▶ ρ -parameter have been obtained by means of
singly subtracted Derivative Dispersion Relations

$$\rho(s) = \frac{1}{\sigma_{tot}(s)} \left\{ \frac{K}{s} + T^R(s) + T^P(s) \right\}$$

- ▶ terms associated with Reggeon R and Pomeron P contributions

$$T^R(s) = -a_1 \tan\left(\frac{\pi b_1}{2}\right) \left[\frac{s}{s_0}\right]^{-b_1} + \tau a_2 \cot\left(\frac{\pi b_2}{2}\right) \left[\frac{s}{s_0}\right]^{-b_2}$$

$$T^P(s) = B \tan\left(\frac{\pi \epsilon}{2}\right) \left[\frac{s}{s_0}\right]^{\epsilon} + \frac{\pi C}{2} + \pi D \ln\left(\frac{s}{s_0}\right)$$

General analytic parametrization

- ▶ Summarizing the General parametrization (10 free fitting parameter)

$$\sigma_{tot}(s) = a_1 \left[\frac{s}{s_0} \right]^{-b_1} + \tau a_2 \left[\frac{s}{s_0} \right]^{-b_2} + A + B \left[\frac{s}{s_0} \right]^e + C \ln \left(\frac{s}{s_0} \right) + D \ln^2 \left(\frac{s}{s_0} \right)$$

$$\begin{aligned} \rho(s) &= \frac{1}{\sigma_{tot}(s)} \left\{ \frac{K}{s} - a_1 \tan \left(\frac{\pi b_1}{2} \right) \left[\frac{s}{s_0} \right]^{-b_1} + \tau a_2 \cot \left(\frac{\pi b_2}{2} \right) \left[\frac{s}{s_0} \right]^{-b_2} \right. \\ &\quad \left. + B \tan \left(\frac{\pi e}{2} \right) \left[\frac{s}{s_0} \right]^e + \frac{\pi C}{2} + \pi D \ln \left(\frac{s}{s_0} \right) \right\} \end{aligned}$$

→ $\tau = -1$ for pp , $\tau = +1$ for $\bar{p}p$ and $s_0 = 4m_p^2 \sim 3.521 \text{ GeV}^2$ (fixed)

General analytic parametrization

- ▶ Encompass some particular analytic structures

Model I: $A = C = D = 0$ (for example, Donnachie and Landshoff)

Model II: $B = C = 0, \epsilon = 0$ (for example, COMPETE and PDG parametrizations)

Model III: $A = B = 0, \epsilon = 0$ (for example, Block-Halzen type)

Model IV: $A = D = 0, \epsilon = 0$ (hybrid power-log)

- ▶ We then construct:

Ensemble TOTEM (T) by adding **only** the TOTEM data in the interval 7 - 13 TeV

Ensemble TOTEM + ATLAS (T + A) by adding **all the TOTEM and ATLAS data** at 7, 8 and 13 TeV

General analytic parametrization

$$\sigma_{tot}(s) = a_1 \left[\frac{s}{s_0} \right]^{-b_1} + \tau a_2 \left[\frac{s}{s_0} \right]^{-b_2} + A + B \left[\frac{s}{s_0} \right]^{\epsilon} + C \ln \left(\frac{s}{s_0} \right) + D \ln^2 \left(\frac{s}{s_0} \right)$$

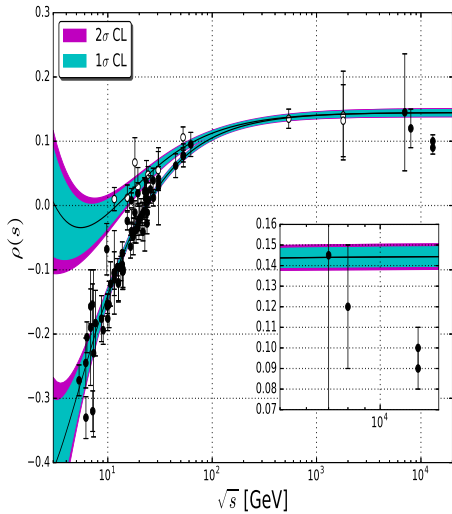
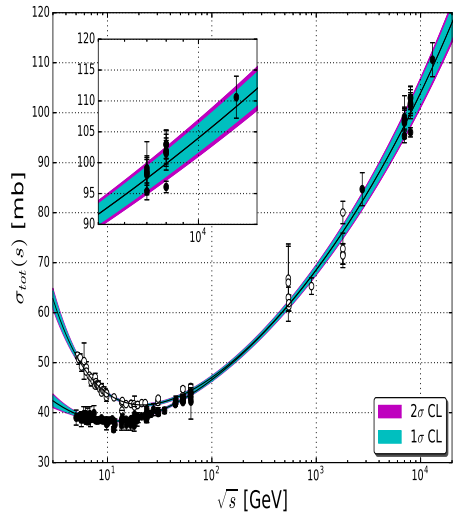
$$\begin{aligned} \rho(s) &= \frac{1}{\sigma_{tot}(s)} \left\{ \frac{K}{s} - a_1 \tan \left(\frac{\pi b_1}{2} \right) \left[\frac{s}{s_0} \right]^{-b_1} + \tau a_2 \cot \left(\frac{\pi b_2}{2} \right) \left[\frac{s}{s_0} \right]^{-b_2} \right. \\ &\quad \left. + B \tan \left(\frac{\pi \epsilon}{2} \right) \left[\frac{s}{s_0} \right]^{\epsilon} + \frac{\pi C}{2} + \pi D \ln \left(\frac{s}{s_0} \right) \right\} \end{aligned}$$

Model I

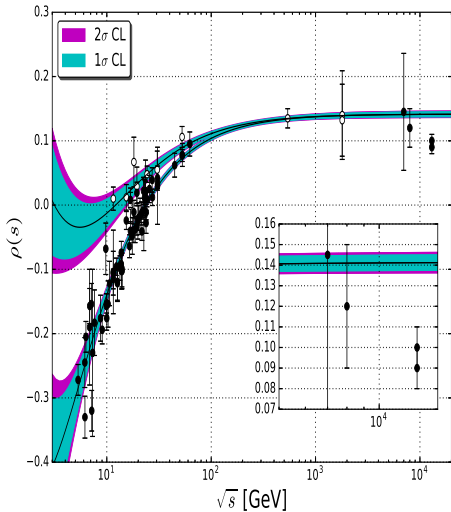
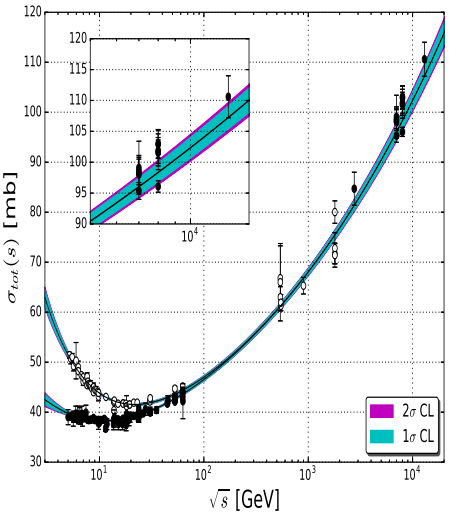
$$\sigma_{tot}(s) = a_1 \left[\frac{s}{s_0} \right]^{-b_1} + \tau a_2 \left[\frac{s}{s_0} \right]^{-b_2} + B \left[\frac{s}{s_0} \right]^{\epsilon}$$

$$\begin{aligned} \rho(s) &= \frac{1}{\sigma_{tot}(s)} \left\{ \frac{K}{s} - a_1 \tan \left(\frac{\pi b_1}{2} \right) \left[\frac{s}{s_0} \right]^{-b_1} + \tau a_2 \cot \left(\frac{\pi b_2}{2} \right) \left[\frac{s}{s_0} \right]^{-b_2} \right. \\ &\quad \left. + B \tan \left(\frac{\pi \epsilon}{2} \right) \left[\frac{s}{s_0} \right]^{\epsilon} \right\} \end{aligned}$$

Model I: Ensemble T



Model I: Ensemble T+A



General analytic parametrization

$$\sigma_{tot}(s) = \textcolor{blue}{a}_1 \left[\frac{s}{s_0} \right]^{-\textcolor{red}{b}_1} + \tau \textcolor{blue}{a}_2 \left[\frac{s}{s_0} \right]^{-\textcolor{red}{b}_2} + \textcolor{blue}{A} + \textcolor{blue}{B} \left[\frac{s}{s_0} \right]^{\textcolor{red}{e}} + \textcolor{blue}{C} \ln \left(\frac{s}{s_0} \right) + \textcolor{blue}{D} \ln^2 \left(\frac{s}{s_0} \right)$$

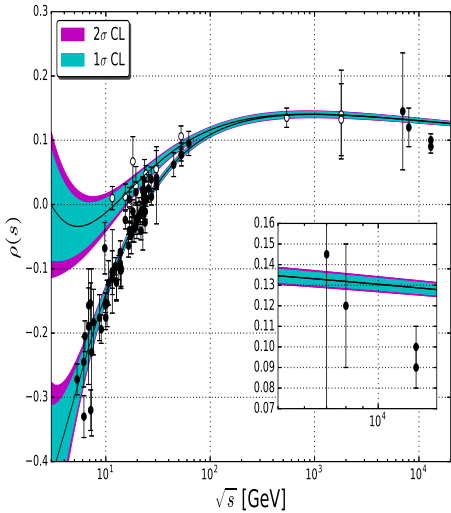
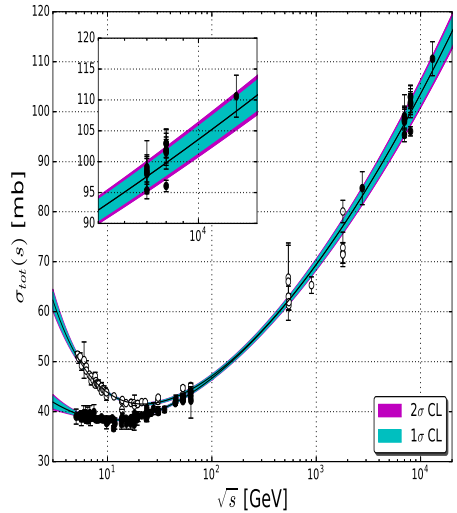
$$\begin{aligned} \rho(s) &= \frac{1}{\sigma_{tot}(s)} \left\{ \frac{\textcolor{red}{K}}{s} - \textcolor{blue}{a}_1 \tan \left(\frac{\pi \textcolor{red}{b}_1}{2} \right) \left[\frac{s}{s_0} \right]^{-\textcolor{red}{b}_1} + \tau \textcolor{blue}{a}_2 \cot \left(\frac{\pi \textcolor{red}{b}_2}{2} \right) \left[\frac{s}{s_0} \right]^{-\textcolor{red}{b}_2} \right. \\ &\quad \left. + \textcolor{blue}{B} \tan \left(\frac{\pi \textcolor{red}{e}}{2} \right) \left[\frac{s}{s_0} \right]^{\textcolor{red}{e}} + \frac{\pi \textcolor{blue}{C}}{2} + \pi \textcolor{blue}{D} \ln \left(\frac{s}{s_0} \right) \right\} \end{aligned}$$

Model II

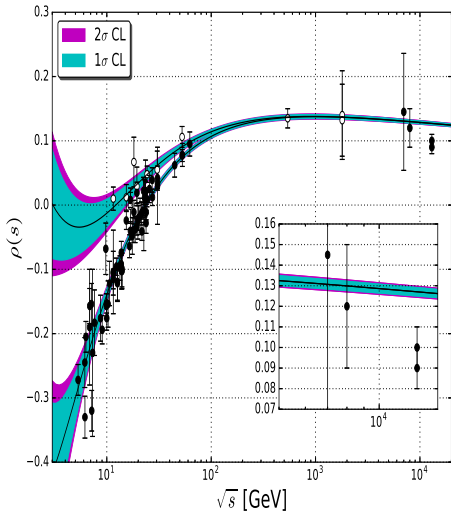
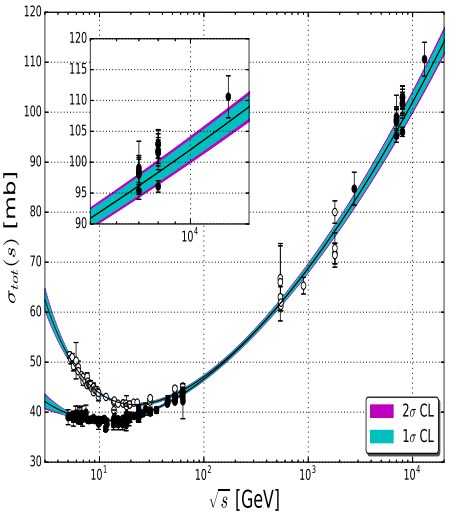
$$\sigma_{tot}(s) = \textcolor{brown}{a}_1 \left[\frac{s}{s_0} \right]^{-\textcolor{brown}{b}_1} + \tau \textcolor{brown}{a}_2 \left[\frac{s}{s_0} \right]^{-\textcolor{brown}{b}_2} + \textcolor{brown}{A} + \textcolor{brown}{D} \ln^2 \left(\frac{s}{s_0} \right)$$

$$\rho(s) = \frac{1}{\sigma_{tot}(s)} \left\{ \frac{\textcolor{brown}{K}}{s} - \textcolor{brown}{a}_1 \tan \left(\frac{\pi \textcolor{brown}{b}_1}{2} \right) \left[\frac{s}{s_0} \right]^{-\textcolor{brown}{b}_1} + \tau \textcolor{brown}{a}_2 \cot \left(\frac{\pi \textcolor{brown}{b}_2}{2} \right) \left[\frac{s}{s_0} \right]^{-\textcolor{brown}{b}_2} + \pi \textcolor{brown}{D} \ln \left(\frac{s}{s_0} \right) \right\}$$

Model II: Ensemble T



Model II: Ensemble T+A



General analytic parametrization

$$\sigma_{tot}(s) = a_1 \left[\frac{s}{s_0} \right]^{-b_1} + \tau a_2 \left[\frac{s}{s_0} \right]^{-b_2} + A + B \left[\frac{s}{s_0} \right]^{\epsilon} + C \ln \left(\frac{s}{s_0} \right) + D \ln^2 \left(\frac{s}{s_0} \right)$$

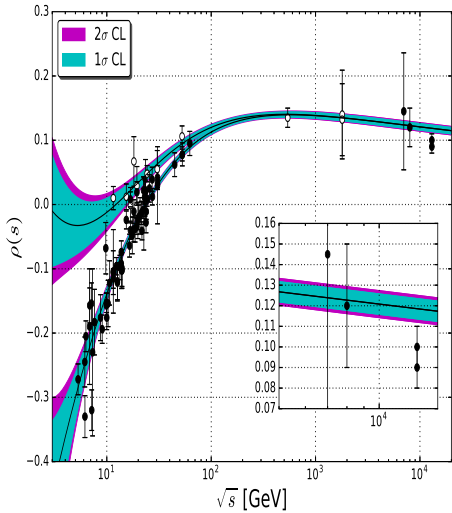
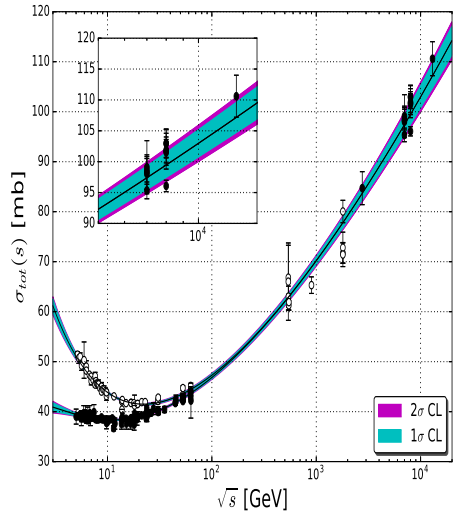
$$\begin{aligned} \rho(s) &= \frac{1}{\sigma_{tot}(s)} \left\{ \frac{K}{s} - a_1 \tan \left(\frac{\pi b_1}{2} \right) \left[\frac{s}{s_0} \right]^{-b_1} + \tau a_2 \cot \left(\frac{\pi b_2}{2} \right) \left[\frac{s}{s_0} \right]^{-b_2} \right. \\ &\quad \left. + B \tan \left(\frac{\pi \epsilon}{2} \right) \left[\frac{s}{s_0} \right]^{\epsilon} + \frac{\pi C}{2} + \pi D \ln \left(\frac{s}{s_0} \right) \right\} \end{aligned}$$

Model III

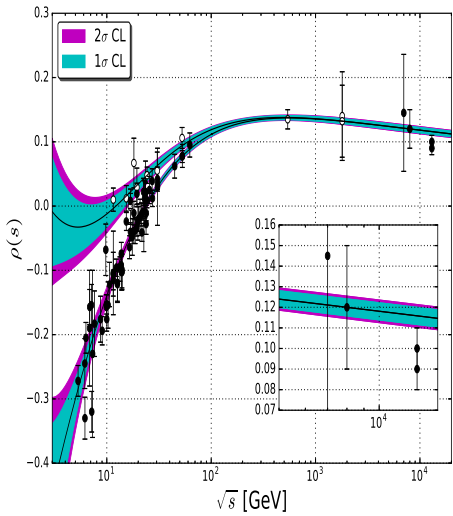
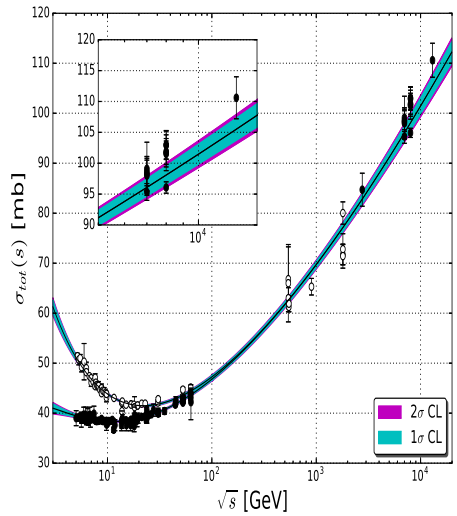
$$\sigma_{tot}(s) = \textcolor{brown}{a}_1 \left[\frac{s}{s_0} \right]^{-\textcolor{brown}{b}_1} + \tau \textcolor{brown}{a}_2 \left[\frac{s}{s_0} \right]^{-\textcolor{brown}{b}_2} + \textcolor{brown}{C} \ln \left(\frac{s}{s_0} \right) + \textcolor{brown}{D} \ln^2 \left(\frac{s}{s_0} \right)$$

$$\begin{aligned} \rho(s) = & \frac{1}{\sigma_{tot}(s)} \left\{ \frac{\textcolor{brown}{K}}{s} - \textcolor{brown}{a}_1 \tan \left(\frac{\pi \textcolor{brown}{b}_1}{2} \right) \left[\frac{s}{s_0} \right]^{-\textcolor{brown}{b}_1} + \tau \textcolor{brown}{a}_2 \cot \left(\frac{\pi \textcolor{brown}{b}_2}{2} \right) \left[\frac{s}{s_0} \right]^{-\textcolor{brown}{b}_2} \right. \\ & \left. + \frac{\pi \textcolor{brown}{C}}{2} + \pi \textcolor{brown}{D} \ln \left(\frac{s}{s_0} \right) \right\} \end{aligned}$$

Model III: Ensemble T



Model III: Ensemble T+A



General analytic parametrization

$$\sigma_{tot}(s) = a_1 \left[\frac{s}{s_0} \right]^{-b_1} + \tau a_2 \left[\frac{s}{s_0} \right]^{-b_2} + A + B \left[\frac{s}{s_0} \right]^{\epsilon} + C \ln \left(\frac{s}{s_0} \right) + D \ln^2 \left(\frac{s}{s_0} \right)$$

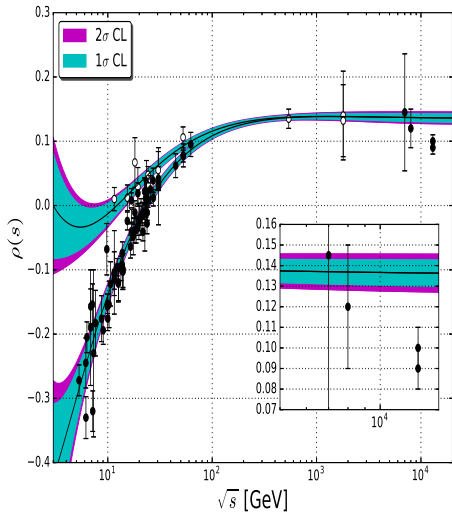
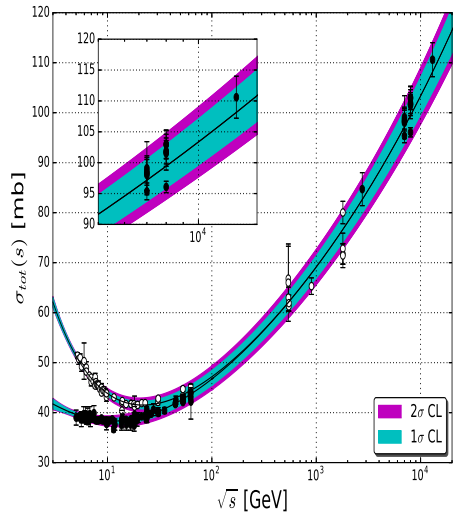
$$\begin{aligned} \rho(s) &= \frac{1}{\sigma_{tot}(s)} \left\{ \frac{K}{s} - a_1 \tan \left(\frac{\pi b_1}{2} \right) \left[\frac{s}{s_0} \right]^{-b_1} + \tau a_2 \cot \left(\frac{\pi b_2}{2} \right) \left[\frac{s}{s_0} \right]^{-b_2} \right. \\ &\quad \left. + B \tan \left(\frac{\pi \epsilon}{2} \right) \left[\frac{s}{s_0} \right]^{\epsilon} + \frac{\pi C}{2} + \pi D \ln \left(\frac{s}{s_0} \right) \right\} \end{aligned}$$

Model IV

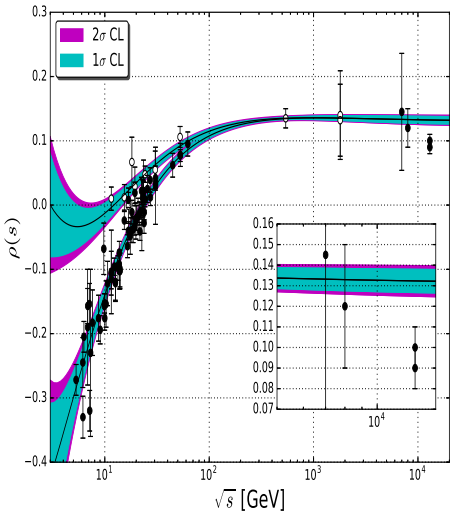
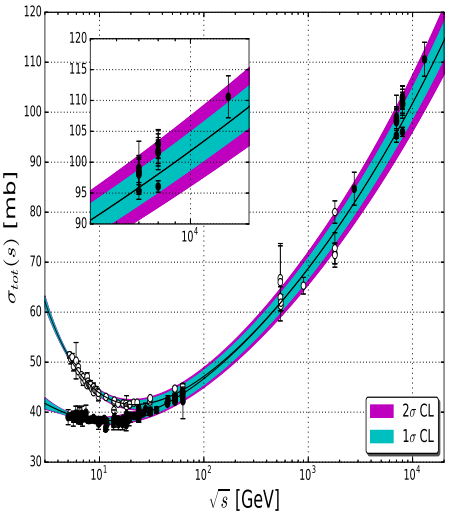
$$\sigma_{tot}(s) = \textcolor{brown}{a}_1 \left[\frac{s}{s_0} \right]^{-\textcolor{brown}{b}_1} + \tau \textcolor{brown}{a}_2 \left[\frac{s}{s_0} \right]^{-\textcolor{brown}{b}_2} + \textcolor{brown}{B} \left[\frac{s}{s_0} \right]^{\epsilon} + \textcolor{brown}{C} \ln \left(\frac{s}{s_0} \right)$$

$$\begin{aligned} \rho(s) &= \frac{1}{\sigma_{tot}(s)} \left\{ \frac{K}{s} - \textcolor{brown}{a}_1 \tan \left(\frac{\pi \textcolor{brown}{b}_1}{2} \right) \left[\frac{s}{s_0} \right]^{-\textcolor{brown}{b}_1} + \tau \textcolor{brown}{a}_2 \cot \left(\frac{\pi \textcolor{brown}{b}_2}{2} \right) \left[\frac{s}{s_0} \right]^{-\textcolor{brown}{b}_2} \right. \\ &\quad \left. + \textcolor{brown}{B} \tan \left(\frac{\pi \epsilon}{2} \right) \left[\frac{s}{s_0} \right]^{\epsilon} + \frac{\pi \textcolor{brown}{C}}{2} \right\} \end{aligned}$$

Model IV: Ensemble T



Model IV: Ensemble T+A



Results: Ensemble T

Model:	I	II	III	IV
a_1 [mb]	41.4 ± 1.8	32.2 ± 1.8	58.8 ± 1.5	51.5 ± 7.1
b_1	0.378 ± 0.028	0.392 ± 0.049	0.229 ± 0.017	0.296 ± 0.037
a_2 [mb]	17.0 ± 2.0	17.0 ± 2.1	16.9 ± 2.0	17.0 ± 2.1
b_2	0.545 ± 0.037	0.545 ± 0.037	0.543 ± 0.036	0.544 ± 0.037
A [mb]	-	29.6 ± 1.2	-	-
B [mb]	21.62 ± 0.73	-	-	9.6 ± 7.5
ϵ	0.0914 ± 0.0030	-	-	0.108 ± 0.019
C [mb]	-	-	3.67 ± 0.34	2.4 ± 1.6
D [mb]	-	0.251 ± 0.010	0.132 ± 0.024	-
K [mbGeV 2]	69 ± 47	55 ± 50	20 ± 44	45 ± 47
ν	248	248	248	247
χ^2/ν	1.273	1.193	1.210	1.249
$P(\chi^2)$	2.3×10^{-3}	2.0×10^{-2}	1.4×10^{-2}	4.8×10^{-3}

Fit results by considering one standard deviation and energy cutoff at 5 GeV.

Results: Ensemble T+A

Model:	I	II	III	IV
a_1 [mb]	41.4 ± 1.8	32.3 ± 2.0	59.1 ± 1.5	53.1 ± 9.6
b_1	0.386 ± 0.028	0.412 ± 0.045	0.234 ± 0.016	0.291 ± 0.044
a_2 [mb]	17.0 ± 2.1	17.0 ± 2.0	16.9 ± 2.0	17.0 ± 2.1
b_2	0.545 ± 0.037	0.545 ± 0.036	0.543 ± 0.036	0.544 ± 0.038
A [mb]	-	30.20 ± 0.90	-	-
B [mb]	22.01 ± 0.64	-	-	8.0 ± 10
ϵ	0.0895 ± 0.0024	-	-	0.110 ± 0.033
C [mb]	-	-	3.81 ± 0.30	2.8 ± 2.1
D [mb]	-	0.244 ± 0.077	0.119 ± 0.020	-
K [mbGeV 2]	73 ± 48	64 ± 50	23 ± 43	46 ± 48
ν	250	250	250	249
χ^2/ν	1.307	1.227	1.234	1.273
$P(\chi^2)$	7.9×10^{-4}	8.2×10^{-3}	6.9×10^{-3}	2.3×10^{-3}

Fit results by considering one standard deviation and energy cutoff at 5 GeV.

Theoretical uncertainty propagation

- ▶ General formula:

$$\begin{aligned}\sigma_w^2(x, y, z, \dots) = & \left(\frac{\partial w}{\partial x} \right)^2 \sigma_x^2 + \left(\frac{\partial w}{\partial y} \right)^2 \sigma_y^2 + \left(\frac{\partial w}{\partial z} \right)^2 \sigma_z^2 + \dots \\ & + 2 \left(\frac{\partial w}{\partial x} \right) \left(\frac{\partial w}{\partial y} \right) \sigma_{xy}^2 + 2 \left(\frac{\partial w}{\partial x} \right) \left(\frac{\partial w}{\partial z} \right) \sigma_{xz}^2 + 2 \left(\frac{\partial w}{\partial y} \right) \left(\frac{\partial w}{\partial z} \right) \sigma_{yz}^2 + \dots\end{aligned}$$

Theoretical uncertainty propagation

- ▶ General formula:

$$\begin{aligned}\sigma_w^2(x, y, z, \dots) &= \left(\frac{\partial w}{\partial x}\right)^2 \sigma_x^2 + \left(\frac{\partial w}{\partial y}\right)^2 \sigma_y^2 + \left(\frac{\partial w}{\partial z}\right)^2 \sigma_z^2 + \dots \\ &+ 2 \left(\frac{\partial w}{\partial x}\right) \left(\frac{\partial w}{\partial y}\right) \sigma_{xy}^2 + 2 \left(\frac{\partial w}{\partial x}\right) \left(\frac{\partial w}{\partial z}\right) \sigma_{xz}^2 + 2 \left(\frac{\partial w}{\partial y}\right) \left(\frac{\partial w}{\partial z}\right) \sigma_{yz}^2 + \dots\end{aligned}$$

- ▶ Total cross section:

$$\sigma_{\sigma_{tot}}^2(s; i, j) = \sum_{i,j} \left(\frac{\partial \sigma_{tot}(s)}{\partial i}\right) \left(\frac{\partial \sigma_{tot}(s)}{\partial j}\right) \sigma_{ij}^2$$

Theoretical uncertainty propagation

- ▶ General formula:

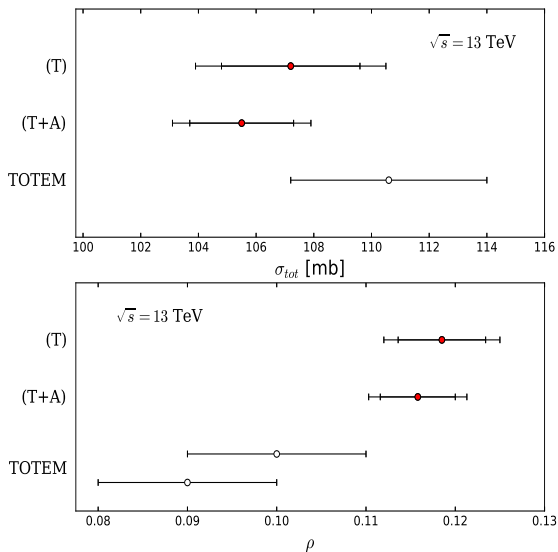
$$\begin{aligned}\sigma_w^2(x, y, z, \dots) &= \left(\frac{\partial w}{\partial x}\right)^2 \sigma_x^2 + \left(\frac{\partial w}{\partial y}\right)^2 \sigma_y^2 + \left(\frac{\partial w}{\partial z}\right)^2 \sigma_z^2 + \dots \\ &+ 2 \left(\frac{\partial w}{\partial x}\right) \left(\frac{\partial w}{\partial y}\right) \sigma_{xy}^2 + 2 \left(\frac{\partial w}{\partial x}\right) \left(\frac{\partial w}{\partial z}\right) \sigma_{xz}^2 + 2 \left(\frac{\partial w}{\partial y}\right) \left(\frac{\partial w}{\partial z}\right) \sigma_{yz}^2 + \dots\end{aligned}$$

- ▶ Total cross section:

$$\sigma_{\sigma_{tot}}^2(s; i, j) = \sum_{i,j} \left(\frac{\partial \sigma_{tot}(s)}{\partial i} \right) \left(\frac{\partial \sigma_{tot}(s)}{\partial j} \right) \sigma_{ij}^2$$

- ▶ ρ -parameter:

$$\sigma_\rho^2(s; i, j) = \frac{1}{\sigma_{tot}^2(s)} \sum_{i,j} \left(\frac{\partial A^R(s; i, j)}{\partial i} - \rho(s) \frac{\partial \sigma_{tot}(s)}{\partial i} \right) \left(\frac{\partial A^R(s; i, j)}{\partial j} - \rho(s) \frac{\partial \sigma_{tot}(s)}{\partial j} \right) \sigma_{ij}^2$$



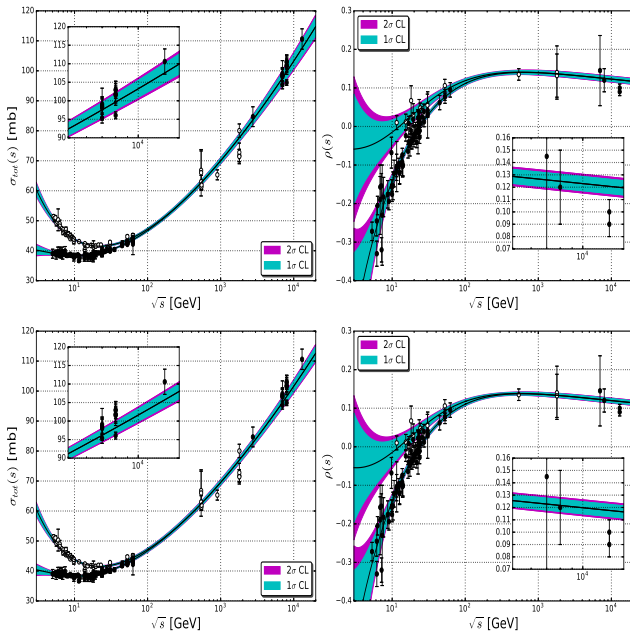
Predictions of Model III for σ_{tot} and ρ at 13 TeV with 1 and 2 standard deviations from fits to ensemble T and T + A together with the TOTEM measurements.

Further tests: Rising the energy cutoff in Model III

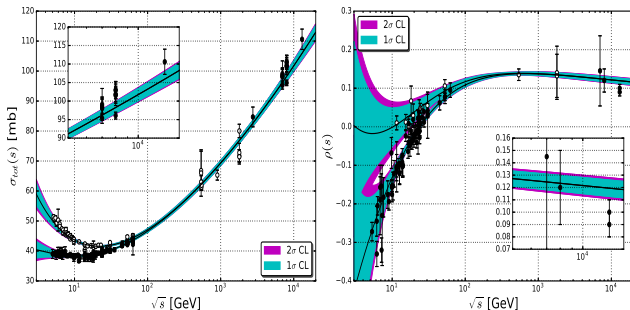
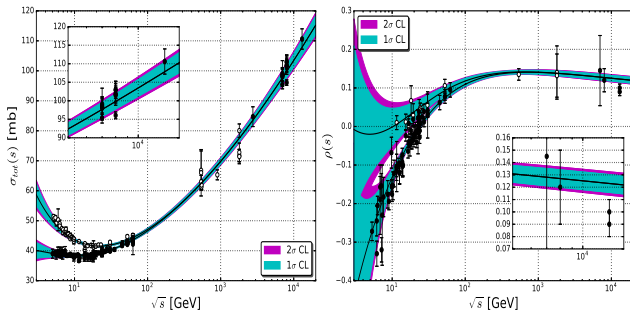
Ensemble:	T		T+A	
	7.5	10	7.5	10
$\sqrt{s_{min}}$ (GeV)				
a_1 [mb]	57.5 ± 2.1	55.8 ± 4.0	57.9 ± 2.1	56.5 ± 4.1
b_1	0.217 ± 0.023	0.202 ± 0.037	0.224 ± 0.021	0.212 ± 0.037
a_2 [mb]	16.8 ± 2.7	15.1 ± 4.6	16.8 ± 2.7	15.1 ± 4.8
b_2	0.542 ± 0.046	0.520 ± 0.070	0.542 ± 0.046	0.520 ± 0.072
C [mb]	3.48 ± 0.44	3.25 ± 0.66	3.66 ± 0.38	3.48 ± 0.59
D [mb]	0.143 ± 0.030	0.156 ± 0.040	0.128 ± 0.024	0.138 ± 0.035
K [mbGeV 2]	-15 ± 74	4.17 ± 116	-9.5 ± 73	14.3 ± 117
ν	205	164	207	166
χ^2/ν	1.217	1.213	1.253	1.263
$P(\chi^2)$	1.8×10^{-2}	3.3×10^{-2}	7.8×10^{-3}	1.2×10^{-2}

Fit results by considering one standard deviation and energy cutoff at 7.5 and 10 GeV.

$\sqrt{s_{min}} = 7.5$ GeV: T above and T+A below



$\sqrt{s_{min}} = 10$ GeV: T above and T+A below

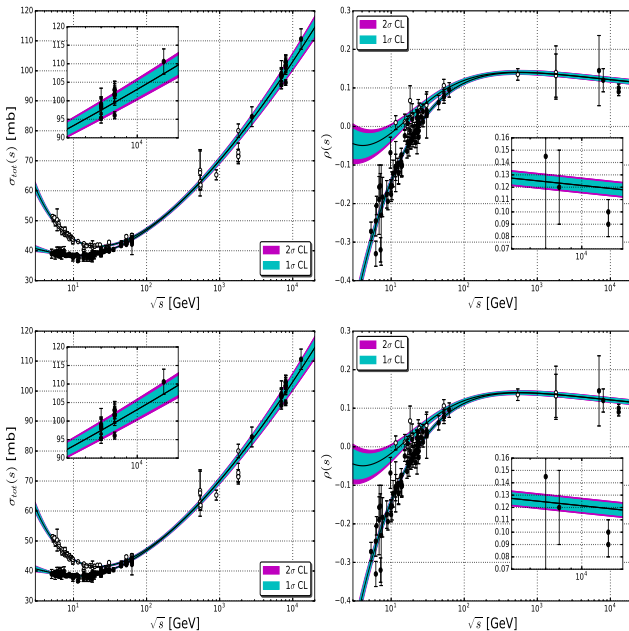


Further tests: Fixing $K = 0$ in Model III

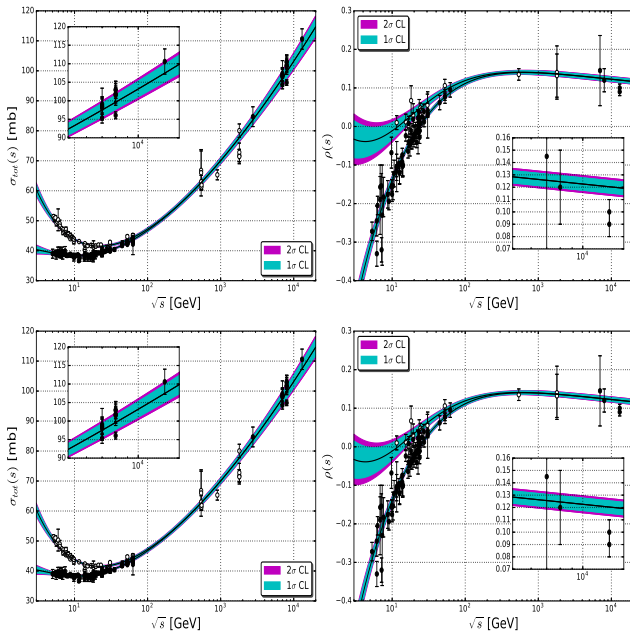
Ensemble:	T			T+A		
	5	7.5	10	5	7.5	10
$\sqrt{s_{min}}$ [GeV]						
a_1 [mb]	58.6 ± 1.3	57.7 ± 1.8	55.8 ± 3.1	58.8 ± 1.3	58.0 ± 1.8	56.2 ± 3.1
b_1	0.226 ± 0.015	0.219 ± 0.019	0.202 ± 0.029	0.231 ± 0.014	0.225 ± 0.018	0.209 ± 0.028
a_2 [mb]	17.0 ± 1.8	16.6 ± 2.3	15.2 ± 4.2	17.1 ± 1.8	16.6 ± 2.3	15.3 ± 4.3
b_2	0.547 ± 0.032	0.538 ± 0.038	0.521 ± 0.064	0.548 ± 0.032	0.539 ± 0.038	0.522 ± 0.063
C [mb]	3.62 ± 0.30	3.51 ± 0.38	3.24 ± 0.53	3.76 ± 0.26	3.67 ± 0.33	3.44 ± 0.47
D [mb]	0.135 ± 0.022	0.141 ± 0.026	0.157 ± 0.033	0.122 ± 0.018	0.127 ± 0.021	0.140 ± 0.029
ν	249	206	165	251	208	167
χ^2/ν	1.210	1.213	1.206	1.238	1.248	1.256
$P(\chi^2)$	1.3×10^{-2}	2.0×10^{-2}	3.7×10^{-2}	6.1×10^{-3}	8.8×10^{-3}	1.4×10^{-2}

Fit results by considering one standard deviation with $K = 0$ (fixed) and energy cutoff at 5, 7.5 and 10 GeV.

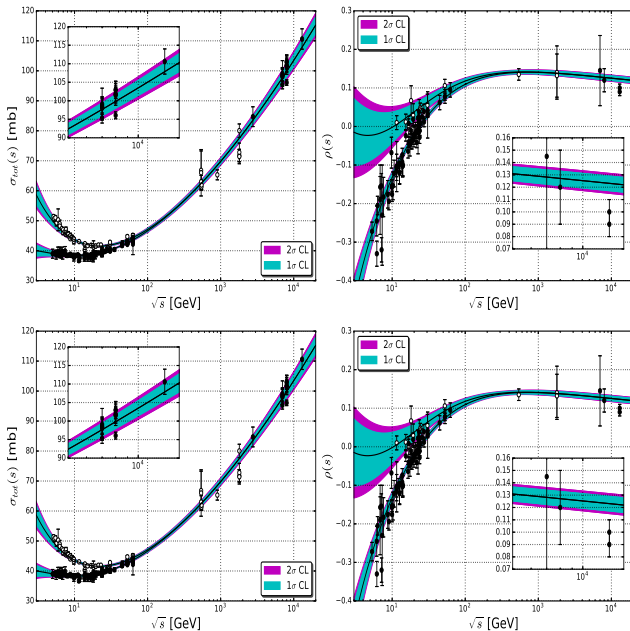
$K = 0$ and $\sqrt{s_{min}} = 5$ GeV: T above and T+A below



$K = 0$ and $\sqrt{s_{min}} = 7.5$ GeV: T above and T+A below



$K = 0$ and $\sqrt{s_{min}} = 10$ GeV: T above and T+A below



Then?

- ▶ Rising the cutoff does not lead to improvements, neither fixing $K = 0$
- ▶ Based on the fit results and taking into account both, **theoretical and experimental uncertainties**, **model III may not be excluded** by the bulk of experimental data
- ▶ Model III with **cutoff at 5 GeV** and **K free** was selected as the best result
- ▶ Notice that this **model III parametrization**, **may not be the best representative approach for a Pomerom model in forward scattering**
- ▶ The main point was to show that even a **simple parametrization**, with only 6 or 7 free fit parameter and even (under crossing) leading contributions, **may not be excluded in fits to a dataset including all the experimental information** that have been obtained at the LHC on σ_{tot} and ρ .

Then?

- ▶ Rising the cutoff does not lead to improvements, neither fixing $K = 0$
- ▶ Based on the fit results and taking into account both, [theoretical and experimental uncertainties](#), [model III may not be excluded](#) by the bulk of experimental data
- ▶ Model III with [cutoff at 5 GeV](#) and [K free](#) was selected as the best result
- ▶ Notice that this [model III parametrization](#), [may not be the best representative approach for a Pomerom model in forward scattering](#)
- ▶ The main point was to show that even a [simple parametrization](#), with only 6 or 7 free fit parameter and even (under crossing) leading contributions, [may not be excluded in fits to a dataset including all the experimental information](#) that have been obtained at the LHC on σ_{tot} and ρ .

\sqrt{s} [TeV]	Ensemble	σ_{tot} (mb)			ρ		
		Central	1σ	2σ	Central	1σ	2σ
13	T	107.2	± 2.4	± 3.3	0.1185	± 0.0049	± 0.0065
	T+A	105.5	± 1.8	± 2.4	0.1158	± 0.0042	± 0.0055
14	T	108.4	± 2.5	± 3.3	0.1179	± 0.0049	± 0.0065
	T+A	106.7	± 1.8	± 2.5	0.1152	± 0.0042	± 0.0055

Reggeon calculus: Survival package

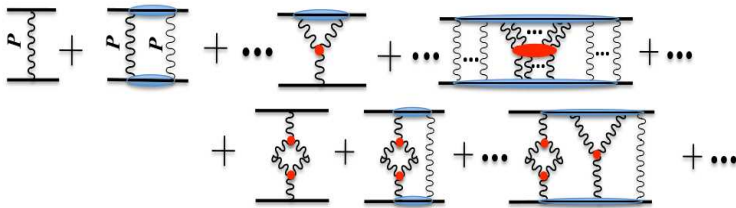
- ▶ Pomeron: from fits to forward observables ($t \approx 0$) → soft Pomeron
- ▶ General unitarity arguments constrain $\alpha_P(0) \leq 1$
- ▶ Observed increase of HE hadronic $\sigma_{tot}(s) \rightarrow \alpha_P(0) = 1 + \epsilon$, with $\epsilon > 0$
- ▶ At high energies:

Reggeon calculus: Survival package

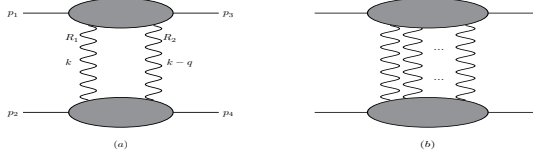
- ▶ Pomeron: from fits to forward observables ($t \approx 0$) → soft Pomeron
- ▶ General unitarity arguments constrain $\alpha_P(0) \leq 1$
- ▶ Observed increase of HE hadronic $\sigma_{tot}(s)$ → ~~$\alpha_P(0) = 1 + \epsilon$, with $\epsilon > 0$~~ **supercritical intercept** →
- ▶ At high energies:

Reggeon calculus: Survival package

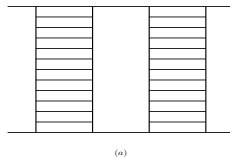
- ▶ Pomeron: from fits to **forward observables** ($t \approx 0$) → soft Pomeron
- ▶ General unitarity arguments constrain $\alpha_P(0) \leq 1$
- ▶ Observed increase of **HE hadronic** $\sigma_{tot}(s) \rightarrow \cancel{\alpha_P(0) = 1 + \epsilon}$, with $\epsilon > 0$ → **supercritical intercept**
- ▶ At high energies:
 - several singularities **closed** to each other
 - take into account their **mutual influence**
 - the **bare Pomeron intercept** may be greater than one



Regge cuts

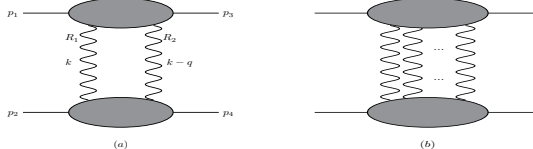


- ▶ Other types of singularity in the ℓ -plane
 - ▶ Important to understand the s -channel unitarity
 - ▶ Interpreted as a set of ladder diagrams

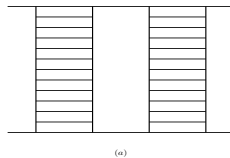


- (a) Independent of the n^{br} of rungs $\rightarrow A(s, t) \underset{s \rightarrow \infty}{\sim} s^{-3} \ln s$

Regge cuts

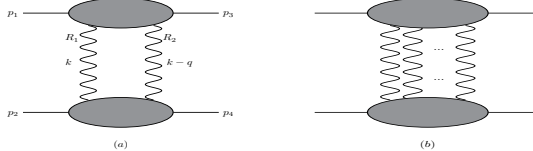


- ▶ Other types of singularity in the ℓ -plane
 - ▶ Important to understand the s -channel unitarity
 - ▶ Interpreted as a set of ladder diagrams

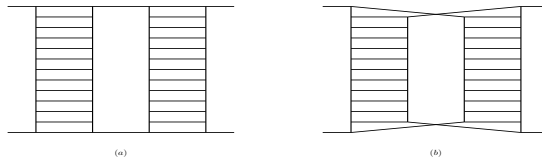


- (a) Independent of the n^{br} of rungs $\rightarrow A(s, t) \underset{s \rightarrow \infty}{\sim} s^{-3} \ln s$ (**Regge pole**)

Regge cuts

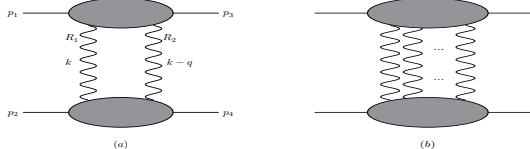


- ▶ Other types of singularity in the ℓ -plane
 - ▶ Important to understand the s -channel unitarity
 - ▶ Interpreted as a set of ladder diagrams

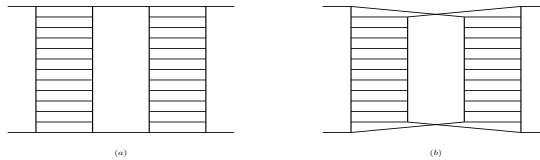


- (a) Independent of the n^{br} of rungs $\rightarrow A(s, t) \underset{s \rightarrow \infty}{\sim} s^{-3} \ln s$ (Regge pole)
 - (b) Branch-cut leading behavior $\rightarrow A(s, t) \underset{s \rightarrow \infty}{\sim} \frac{s^{\alpha_C(t)}}{\ln s}$

Regge cuts



- ▶ Other types of singularity in the ℓ -plane
- ▶ Important to understand the s -channel unitarity
- ▶ Interpreted as a set of ladder diagrams



- (a) Independent of the n^{br} of rungs $\rightarrow A(s, t) \underset{s \rightarrow \infty}{\sim} s^{-3} \ln s$ (**Regge pole**)
- (b) Branch-cut leading behavior $\rightarrow A(s, t) \underset{s \rightarrow \infty}{\sim} \frac{s^{\alpha_C(t)}}{\ln s}$ (**simplest case**)

Multi-reggeon exchange

- ▶ n^{th} -Reggeon exchange amplitude

$$A^{(n)}(s, t) = \frac{i^{n-1}}{n!} \frac{1}{(2s)^{n-1}} (2\pi)^2 \int \prod_{i=1}^n \left[\frac{d^2 \mathbf{k}_{i\perp}}{(2\pi)^2} A^{(1)}(s, \mathbf{k}_{i\perp}) \right] \delta \left(\mathbf{q}_\perp - \sum_{i=1}^n \mathbf{k}_{i\perp} \right)$$

- ▶ By assuming some conditions → e.g. low- $|t|$ values and linear trajectories

$$A^{(n)}(s, t) \sim i^{n-1} \gamma^n(0) \eta^n(0) \frac{s^{n(\alpha(0)-1)+1}}{\Lambda^{n-1}(s)} e^{\Lambda(s)t/n}$$

- where $\Lambda(s) = B_0/2 + \alpha'(\ln s)$, remember that: $(\ln ix = \ln x - i\pi/2)$
- ▶ At the asymptotic limit of high energies

$$A^{(n)}(s, t) \underset{s \rightarrow \infty}{\sim} \frac{s^{\alpha_c(t)}}{\ln^{n-1} s}, \quad \alpha_c(t) = n(\alpha(0) - 1) + 1 + \frac{\alpha'}{n} t$$

- For the case of **n Pomerons**, whose $\alpha_P(t) = \alpha_P^0 + \alpha'_P t$

$$\alpha_c(t) = \alpha_P^0 + \frac{\alpha'_P}{n} t$$

Two-reggeon exchange

- ▶ Simplifying: two-Reggeon exchange amplitude

$$A^{(2)}(s, t) = \frac{i}{2s2!} \int \frac{d^2\mathbf{k}_\perp}{(2\pi)^2} A^{(1)}(s, \mathbf{k}_\perp^2) A^{(1)}(s, (\mathbf{q}_\perp - \mathbf{k}_\perp)^2)$$

- $A^{(1)}$ represents the Regge pole scattering amplitude
- ▶ By considering a typical Regge pole amplitude, one arrives at

$$A^{(2)}(s, t) = \frac{i}{16\pi} \gamma^2(0) \eta^2(0) \frac{s^{2\alpha(0)-1}}{2\Lambda(s)} e^{\Lambda(s)t/2}$$

- cut singularity located at

$$\alpha_c(t) = 2\alpha(0) - 1 + \frac{\alpha'}{2} t$$

- ▶ As for the case of double-Pomeron exchange

$$\sigma_{tot} \sim A s^{\alpha_P(0)-1} - B \frac{s^{2(\alpha_P(0)-1)}}{\ln s}$$

Phenomenology: Born-level analysis

- ▶ The scattering amplitude is decomposed into three terms

$$A_B(s, t) = A_{\mathbb{P}}(s, t) + A_+(s, t) + \tau A_-(s, t)$$

where τ flips sign when going from $pp (\tau = -1)$ to $\bar{p}p (\tau = +1)$

- ▶ leading singularity:
 - $A_{\mathbb{P}}(s, t) \rightarrow$ single **Pomeron** exchange, $\xi = +1$
- ▶ secondary Reggeons:
 - $A_{+(-)}(s, t) \rightarrow$ exchange of the Reggeons with $\xi = +1(-1)$, namely a_2 and f_2 (ω and ρ)
- ▶ For single Regge exchange

$$A_i(s, t) = \beta_i^2(t) \eta_i(t) \left(\frac{s}{s_0} \right)^{\alpha_i(t)}$$

– where $\gamma_i(t) = \beta_i^2(t)$ is the elastic proton-Reggeon vertex, $\alpha_i(t)$ is the Regge pole trajectory, with $i = \mathbb{P}, +, -$

Phenomenology: Born-level analysis

- ▶ Asymptotic form of the signatures at the very low- t region

Phenomenology: Born-level analysis

- ▶ Asymptotic form of the signatures at the very low- t region

$$\eta_i(t) = \underbrace{-e^{-i\pi\alpha_i(t)/2}}_{\xi=+1}$$

Phenomenology: Born-level analysis

- ▶ Asymptotic form of the signatures at the very low- t region

$$\eta_i(t) = \underbrace{-e^{-i\pi\alpha_i(t)/2}}_{\xi=+1} \quad \text{and} \quad \eta_i(t) = \underbrace{ie^{-i\pi\alpha_i(t)/2}}_{\xi=-1}$$

Phenomenology: Born-level analysis

- ▶ Asymptotic form of the signatures at the very low- t region

$$\eta_i(t) = \underbrace{-e^{-i\pi\alpha_i(t)/2}}_{\xi=+1} \quad \text{and} \quad \eta_i(t) = \underbrace{ie^{-i\pi\alpha_i(t)/2}}_{\xi=-1}$$

- ▶ do not affect the Pomeron parameters ϵ and α'_P , but simply introduces the vertex transformations

$$\beta_P^2(t) \rightarrow \sin \left[\frac{\pi}{2} \alpha_P(t) \right] \beta_P^2(t)$$

$$\beta_+^2(t) \rightarrow \sin \left[\frac{\pi}{2} \alpha_+(t) \right] \beta_+^2(t)$$

$$\beta_-^2(t) \rightarrow -\cos \left[\frac{\pi}{2} \alpha_-(t) \right] \beta_-^2(t)$$

Phenomenology: Born-level analysis

By means of these simplified form of the Regge signatures:

- ▶ Pomeron contribution, $\xi = +1$

$$A_P(s, t) = -\beta_P^2(t) \cos \left[\frac{\pi}{2} \alpha_P(t) \right] \left(\frac{s}{s_0} \right)^{\alpha_P(t)} + i \beta_P^2(t) \sin \left[\frac{\pi}{2} \alpha_P(t) \right] \left(\frac{s}{s_0} \right)^{\alpha_P(t)}$$

- ▶ Reggeons with $\xi = +1$

$$A_+(s, t) = -\beta_+^2(t) \cos \left[\frac{\pi}{2} \alpha_+(t) \right] \left(\frac{s}{s_0} \right)^{\alpha_+(t)} + i \beta_+^2(t) \sin \left[\frac{\pi}{2} \alpha_+(t) \right] \left(\frac{s}{s_0} \right)^{\alpha_+(t)}$$

- ▶ Reggeons with $\xi = -1$

$$A_-(s, t) = \beta_-^2(t) \sin \left[\frac{\pi}{2} \alpha_-(t) \right] \left(\frac{s}{s_0} \right)^{\alpha_-(t)} + i \beta_-^2(t) \cos \left[\frac{\pi}{2} \alpha_-(t) \right] \left(\frac{s}{s_0} \right)^{\alpha_-(t)}$$

Phenomenology: Born-level analysis

Secondary Reggeons exchange

- ▶ Positive-signature are taken to have an exponential form for the proton-Reggeon vertex

$$\beta_+(t) = \beta_+(0)\exp(r_+ t/2)$$

- lie on an exchange-degenerate linear trajectory

$$\alpha_+(t) = 1 - \eta_+ + \alpha'_+ t$$

- ▶ Similarly, for the case of the exchange-degenerate negative-signature

$$\beta_-(t) = \beta_-(0)\exp(r_- t/2)$$

$$\alpha_-(t) = 1 - \eta_- + \alpha'_- t$$

Phenomenology: Born-level analysis

Pomeron exchange

it will be investigated two different types of:

- ▶ proton-Pomeron vertex, (one of which being a power-like form):

$$\beta_P(t) = \beta_P(0) \exp(r_P t/2) \quad \text{and} \quad \beta_P(t) = \frac{\beta_P(0)}{(1-t/a_1)(1-t/a_2)}$$

- ▶ trajectories, (one of which being non-linear):

$$\alpha_P(t) = \alpha_P(0) + \alpha'_+ t \quad \text{and} \quad \alpha_P(t) = \alpha_P(0) + \alpha'_P t - \frac{\beta_\pi^2 m_\pi^2}{32\pi^3} h\left(\frac{4m_\pi^2}{|t|}\right)$$

$$h(x) = \frac{4}{x} F_\pi^2(t) \left[2x - (1+x)^{3/2} \ln\left(\frac{\sqrt{1+x}+1}{\sqrt{1+x}-1}\right) + \ln\left(\frac{m^2}{m_\pi^2}\right) \right]$$

- non-linear term → nearest **t-channel** singularity (two-pion loop)
- $m_\pi = 139.6$ MeV and $F_\pi(t) = \beta_\pi/(1-t/a_1)$ stands for the pion-Pomeron vertex
- $\beta_\pi/\beta_P = 2/3$

Phenomenology: Born-level analysis

- ▶ **B I model:**
 - it was adopted an **exponential form** for the **proton-Pomeron vertex** and for the **secondary Reggeons**
 - it was used a ***linear trajectory*** for the **Pomeron**
- ▶ **B II model:**
 - **exponential form** for the **proton-Pomeron vertex** and for the **secondary Reggeons**
 - ***non-linear trajectory*** for the **Pomeron**
- ▶ **B III model:**
 - power-like form for the **proton-Pomeron vertex** and **exponential form** for the **secondary Reggeons**
 - ***non-linear trajectory*** for the **Pomeron**
- ▶ **B IV(=B I+PP) model** (double-Pomeron exchange):
 - power-like form for the **proton-Pomeron vertex** and for the **secondary Reggeons**
 - ***non-linear trajectory*** for the **Pomeron**

Phenomenology: Born-level analysis

Double-Pomeron exchange

- multi-Pomeron exchanges tame the asymptotic rise of cross section → enters, **phenomenologically**, to ensure **unitarity**
 - ▶ PP contribution is negative, at $s \rightarrow \infty$ as $A_{\text{PP}}(s, t) \sim -s^{\alpha_{\text{PP}}(t)} / \ln s$
 - ▶ is flatter in t than the single-Pomeron exchange

$$\alpha_{\text{PP}}(t) = 1 + 2\epsilon + \frac{1}{2} \alpha'_P t$$

- ▶ it was added the phenomenological term to the amplitude

$$A_{\text{PP}}(s, t) = -\beta_{\text{PP}}^2(t) \eta_{\text{PP}}(t) \frac{s^{\alpha_{\text{PP}}(t)}}{s_0} \left[\ln \left(\frac{s}{s_0} \right) \right]^{-1}$$

- where $\eta_{\text{PP}}(t) = -e^{-i\pi\alpha_{\text{PP}}(t)/2}$, $\beta_{\text{PP}} = \exp(r_P t/4)$

Physical observables

- ▶ Total cross section

$$\begin{aligned}\sigma_{tot}(s) &= \frac{4\pi}{s} \operatorname{Im} A(s, t = 0) \\ &= X s^\epsilon + Y_+ s^{-\eta_+} + \tau Y_- s^{-\eta_-}\end{aligned}$$

— where $A(s, t) = A_B(s, t)$ and X and Y_\pm represents the **imaginary part** of the forward scattering amplitude

- ▶ Elastic differential cross section

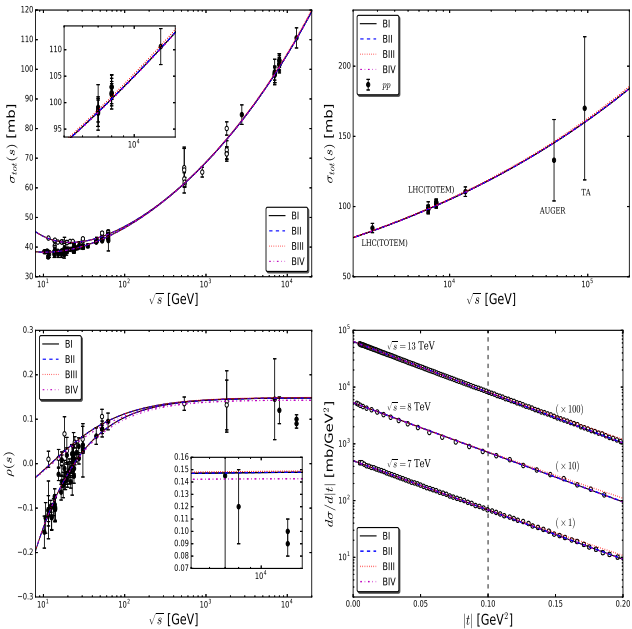
$$\frac{d\sigma}{d|t|}(s, t) = \frac{\pi}{s^2} |\operatorname{Im} A(s, t)|^2$$

- ▶ Ratio of the real to imaginary part of the forward scattering amplitude

$$\rho(s) = \frac{\operatorname{Re} A(s, t = 0)}{\operatorname{Im} A(s, t = 0)}$$

Results: (only TOTEM)

	Born-level amplitudes			
	B I	B II	B III	B IV
ϵ	0.0938 ± 0.0023	0.0938 ± 0.0023	0.0944 ± 0.0025	0.0941 ± 0.0028
α'_P [GeV $^{-2}$]	0.253 ± 0.011	0.252 ± 0.011	0.27 ± 0.16	0.254 ± 0.011
$\beta_P(0)$ [GeV $^{-1}$]	1.962 ± 0.038	1.962 ± 0.038	1.956 ± 0.041	1.958 ± 0.047
b_P [GeV $^{-2}$]	5.5 [fixed]	5.5 [fixed]	-	5.5 [fixed]
η_+	0.344 ± 0.041	0.343 ± 0.041	0.341 ± 0.043	0.335 ± 0.045
α'_+ [GeV $^{-2}$]	0.9 [fixed]	0.9 [fixed]	0.9 [fixed]	0.9 [fixed]
$\beta_+(0)$ [GeV $^{-1}$]	3.77 ± 0.33	3.77 ± 0.33	3.76 ± 0.35	3.70 ± 0.36
b_+ [GeV $^{-2}$]	0.5 [fixed]	0.5 [fixed]	0.5 [fixed]	0.5 [fixed]
η_-	0.530 ± 0.070	0.530 ± 0.070	0.530 ± 0.075	0.543 ± 0.075
α'_- [GeV $^{-2}$]	0.9 [fixed]	0.9 [fixed]	0.9 [fixed]	0.9 [fixed]
$\beta_-(0)$ [GeV $^{-1}$]	2.91 ± 0.43	2.91 ± 0.43	2.91 ± 0.46	2.98 ± 0.47
b_- [GeV $^{-2}$]	3.1 [fixed]	3.1 [fixed]	3.1 [fixed]	3.1 [fixed]
a_1 [GeV 2]	-	m_ρ^2 [fixed]	m_ρ^2 [fixed]	-
a_2 [GeV 2]	-	-	0.90 ± 0.48	-
$\beta_{PP}(0)$ [GeV $^{-1}$]	-	-	-	0.026 ± 0.017
ν	305	305	304	304
χ^2/ν	0.823	0.823	0.831	0.820



Predictions of the forward and nonforward observables in the Born-level analysis.

Phenomenology: Eikonal analysis

- ▶ Breakdown of unitarity can be avoided → the exchange series

$$\mathbb{P} + \mathbb{P}\mathbb{P} + \mathbb{P}\mathbb{P}\mathbb{P} + \dots$$

- ▶ It is not entirely understood how to carry out a **full computation** of them
- ▶ **Pomeron** contribution → **single-exchange** in the Born-level amplitude

Phenomenology: Eikonal analysis

- ▶ Breakdown of unitarity can be avoided → the exchange series

$$\mathbb{P} + \mathbb{P}\mathbb{P} + \mathbb{P}\mathbb{P}\mathbb{P} + \dots$$

- ▶ It is not entirely understood how to carry out a **full computation** of them
- ▶ **Pomeron** contribution → **single-exchange** in the Born-level amplitude
- ▶ Relation **one-to-one**?

Phenomenology: Eikonal analysis

- ▶ Breakdown of unitarity can be avoided → the exchange series

$$\mathbb{P} + \mathbb{P}\mathbb{P} + \mathbb{P}\mathbb{P}\mathbb{P} + \dots$$

- ▶ It is not entirely understood how to carry out a **full computation** of them
- ▶ **Pomeron** contribution → **single-exchange** in the Born-level amplitude
- ▶ Relation **one-to-one?**

$$1 - \sum_{n=0}^{\infty} \frac{(i\chi)^n}{n!} = -i\chi + \chi^2 + i\chi^3 + \dots \leftrightarrow \mathbb{P} + \mathbb{P}\mathbb{P} + \mathbb{P}\mathbb{P}\mathbb{P} + \dots$$

Phenomenology: Eikonal analysis

- ▶ Breakdown of unitarity can be avoided → the exchange series

$$\mathbb{P} + \mathbb{P}\mathbb{P} + \mathbb{P}\mathbb{P}\mathbb{P} + \dots$$

- ▶ It is not entirely understood how to carry out a **full computation** of them
- ▶ **Pomeron** contribution → **single-exchange** in the Born-level amplitude
- ▶ Relation **one-to-one?**

$$1 - \sum_{n=0}^{\infty} \frac{(i\chi)^n}{n!} = -i\chi + \chi^2 + i\chi^3 + \dots \leftrightarrow \mathbb{P} + \mathbb{P}\mathbb{P} + \mathbb{P}\mathbb{P}\mathbb{P} + \dots$$

- ▶ This is not absolutely true → but it is a **phenomenological way** to give some meaning to eikonal unitarization

$$A_B(s, t) = s \int_0^{\infty} db b J_0(b\sqrt{-t}) \chi(s, b)$$

– at first order

Phenomenology: Eikonal analysis

- ▶ eikonalization is an effective procedure to take into account some properties of high-energy s -channel unitarity
- ▶ inverting the Fourier transform

$$\chi(s, b) = \frac{1}{s} \int_0^\infty d\sqrt{-t} \sqrt{-t} J_0(b\sqrt{-t}) A_B(s, t)$$

- the first term in the eikonal series is related to the **single-exchange Born-level amplitude**
- ▶ the “full eikonalized” amplitude

$$A_{eik}(s, t) = is \int_0^\infty db b J_0(b\sqrt{-t}) \left[1 - e^{i\chi(s, b)} \right]$$

– where $\chi(s, b) = \chi_R(s, b) + i\chi_I(s, b)$

Phenomenology: Eikonal analysis

- ▶ eikonalization is an effective procedure to take into account some properties of high-energy s -channel unitarity
- ▶ inverting the Fourier transform

$$\chi(s, b) = \frac{1}{s} \int_0^\infty d\sqrt{-t} \sqrt{-t} J_0(b\sqrt{-t}) A_B(s, t)$$

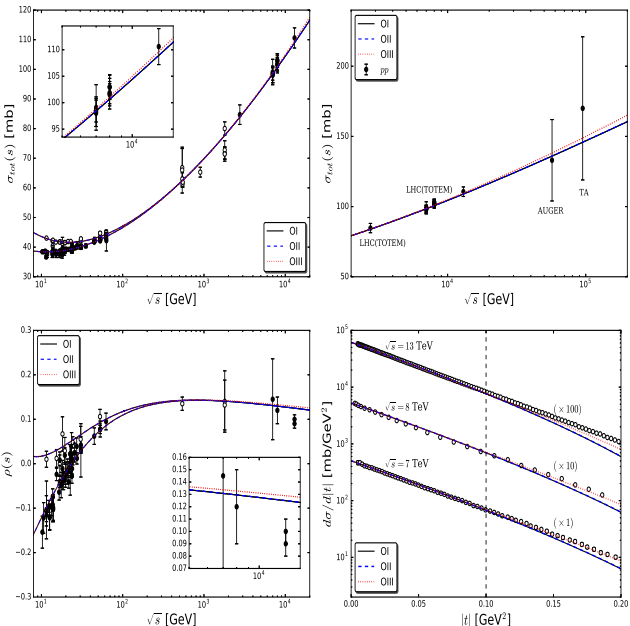
- the first term in the eikonal series is related to the **single-exchange Born-level amplitude**
- ▶ the “full eikonalized” amplitude

$$A_{eik}(s, t) = is \int_0^\infty db b J_0(b\sqrt{-t}) \left[1 - e^{i\chi(s, b)} \right]$$

- where $\chi(s, b) = \chi_R(s, b) + i\chi_I(s, b)$
- ▶ this is ““*a way to take into account*”” the whole multiple-Pomeron exchange

Results: (only TOTEM)

	One-channel eikonalized amplitudes		
	OI	OII	OIII
ϵ	0.1246 ± 0.0014	0.124620 ± 0.000090	0.1250 ± 0.0033
α'_P [GeV $^{-2}$]	0.03005 ± 0.00030	0.0300 ± 0.0087	0.09018 ± 0.00033
$\beta_P(0)$ [GeV $^{-1}$]	1.827 ± 0.010	1.826 ± 0.019	1.858 ± 0.053
b_P [GeV $^{-2}$]	7.2690 ± 0.0011	7.24 ± 0.48	-
η_+	0.2992 ± 0.0067	0.299 ± 0.016	0.307 ± 0.038
α'_+ [GeV $^{-2}$]	0.9 [fixed]	0.9 [fixed]	0.9 [fixed]
$\beta_+(0)$ [GeV $^{-1}$]	4.288 ± 0.010	4.286 ± 0.034	4.42 ± 0.34
b_+ [GeV $^{-2}$]	0.5 [fixed]	0.5 [fixed]	0.5 [fixed]
η_-	0.5398 ± 0.0041	0.539 ± 0.018	0.541 ± 0.072
α'_- [GeV $^{-2}$]	0.9 [fixed]	0.9 [fixed]	0.9 [fixed]
$\beta_-(0)$ [GeV $^{-1}$]	3.557 ± 0.030	3.55 ± 0.13	3.60 ± 0.53
b_- [GeV $^{-2}$]	3.1 [fixed]	3.1 [fixed]	3.1 [fixed]
a_1 [GeV 2]	-	m_ρ^2 [fixed]	m_ρ^2 [fixed]
a_2 [GeV 2]	-	-	0.1250 ± 0.0033
ν	304	304	304
χ^2/ν	0.807	0.807	0.823



Predictions of the forward and nonforward observables in the one-channel eikonalized analysis.

Phenomenology: Eikonal analysis

Double-channel eikonal analysis

- ▶ Diffractive proton excitation in intermediate states
- ▶ two-channel eikonal approach → by means of the Good-Walker formalism
 - convenient way to incorporate $p \rightarrow N^*$ diffractive dissociation

$$\beta_p \rightarrow \begin{pmatrix} \beta_p(p \rightarrow p) & \beta_p(p \rightarrow N^*) \\ \beta_p(N^* \rightarrow p) & \beta_p(N^* \rightarrow N^*) \end{pmatrix} \simeq \beta(p \rightarrow p) \begin{pmatrix} 1 & \gamma \\ \gamma & 1 \end{pmatrix}$$

- ▶ Pomeron couplings

$$\beta_{P,k}(t) = (1 \pm \gamma) \beta_P(t)$$

- where $1 \pm \gamma$ stands for the eigenvalues of the two-channel vertex, with $\gamma \simeq 0.55$

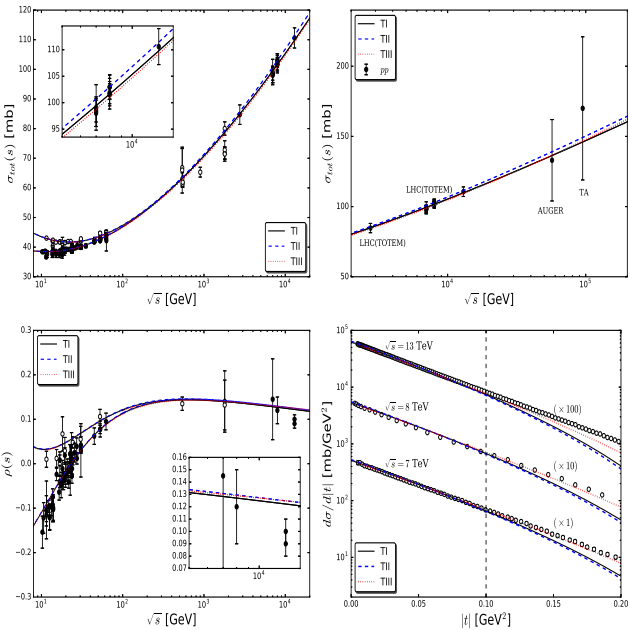
→ associated with excitations into particular channels with $\sigma_{SD}^{lowM} \simeq 2$ mb at $\sqrt{s} = 31$ GeV

- ▶ each amplitude has two vertices

$$A_{eik}(s, t) = is \int_0^\infty b db J_0(bq) \left[1 - \frac{1}{4} e^{i(1+\gamma)^2 \chi(s,b)} - \frac{1}{2} e^{i(1+\gamma^2) \chi(s,b)} - \frac{1}{4} e^{i(1-\gamma)^2 \chi(s,b)} \right]$$

Results: (only TOTEM)

	Two-channel eikonalized amplitudes		
	DI	DII	DIII
ϵ	0.1505 ± 0.0048	0.1508 ± 0.0048	0.1535 ± 0.0016
α'_P [GeV $^{-2}$]	0.0100 ± 0.0022	0.0208 ± 0.0066	0.019 ± 0.016
$\beta_P(0)$ [GeV $^{-1}$]	1.737 ± 0.075	1.734 ± 0.074	1.776 ± 0.030
b_P [GeV $^{-2}$]	6.61 ± 0.31	6.58 ± 0.18	-
η_+	0.289 ± 0.039	0.2875 ± 0.0039	0.2983 ± 0.0039
α'_+ [GeV $^{-2}$]	0.9 [fixed]	0.9 [fixed]	0.9 [fixed]
$\beta_+(0)$ [GeV $^{-1}$]	4.86 ± 0.36	4.85 ± 0.36	5.034 ± 0.013
b_+ [GeV $^{-2}$]	0.5 [fixed]	0.5 [fixed]	0.5 [fixed]
η_-	0.543 ± 0.069	0.543 ± 0.070	0.545 ± 0.057
α'_- [GeV $^{-2}$]	0.9 [fixed]	0.9 [fixed]	0.9 [fixed]
$\beta_-(0)$ [GeV $^{-1}$]	4.03 ± 0.58	4.03 ± 0.58	4.08 ± 0.48
b_- [GeV $^{-2}$]	3.1 [fixed]	3.1 [fixed]	3.1 [fixed]
a_1 [GeV 2]	-	m_ρ^2 [fixed]	m_ρ^2 [fixed]
a_2 [GeV 2]	-	-	0.80 ± 0.19
ν	304	304	304
χ^2/ν	0.896	0.895	0.892



Predictions of the forward and nonforward observables in the two-channel eikonalized analysis.

Conclusions

- ▶ Tension between the **TOTEM** and **ATLAS** measurements
 - different scenarios for the rise of σ_{tot} → soft Pomeron parameters
- ▶ We understand → forward ensemble must be **TOTEM + ATLAS**
 - However, **ATLAS** measurements may cause some bias
- ▶ $\alpha_P(0) = 1 + \epsilon$ is valid over a limited energy-range.
 - ϵ represents **more than only** single Pomeron exchange
- * **Born-level:** smooth differences mainly due to the power-like $p - \mathbb{P}$ vertex
 - nonlinear $\alpha_P(t)$ → not sufficient to play a substantial statistical weight
 - **BI** are indistinguishable from **BII**, and very close to **BIII** and **BI+P**
- ** **One-channel:** practically no difference between **OI** and **OII**, i.e. nonlinear $\alpha_P(t)$ again not sufficient?
 - **OIII** → power-like vertex
- *** **Two-channel:** σ_{tot} for **TI** and **TII** are very similar, whilst for ρ there is practically no difference between **TII** and **TIII**
- ▶ In all the 3-kinds of analysis: σ_{tot} are well-described, but that's not the case for ρ and σ_{el}^{diff} are reasonable good up to $t \leq 0.1 \text{ GeV}^2$

Quantum Chromodynamics

QCD: Basics

- ▶ Describes the strong interactions among quarks (ψ_q) and gluons (G_μ^A)
- ▶ invariant properties of the symmetry group $SU(N_c)$, $N_c = 3$

$$[\lambda^A, \lambda^B] = if^{ABC} \lambda^C$$

- ▶ Lagrangian

$$\mathcal{L}_{QCD} = -\frac{1}{4} F_{\mu\nu}^A(x) F_A^{\mu\nu}(x) + \sum_q \bar{\psi}_q^r(x) (iD^\mu - m)_{rs} \psi_q^s(x) + \mathcal{L}_{gauge-fixing} + \mathcal{L}_{ghost}$$

- where $F_{\mu\nu}^A = \partial_\mu G_\nu^A - \partial_\nu G_\mu^A - g_s f^{ABC} G_\mu^B G_\nu^C$
- $f_{ABE} f_{ECD} + f_{CBE} f_{AED} + f_{DBE} f_{ACE} = 0$
- g_s is the strong coupling

QCD: Basics

- ▶ Describes the strong interactions among **quarks** (ψ_q) and **gluons** (G_μ^A)
- ▶ invariant properties of the symmetry group $SU(N_c)$, $N_c = 3$

$$[\lambda^A, \lambda^B] = i f^{ABC} \lambda^C$$

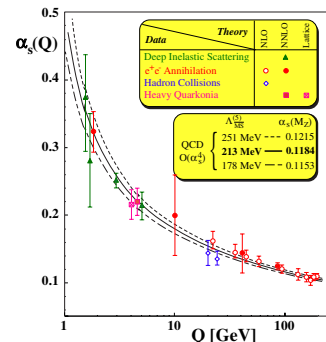
- ▶ Lagrangian

$$\mathcal{L}_{QCD} = -\frac{1}{4} F_{\mu\nu}^A(x) F_A^{\mu\nu}(x) + \sum_q \bar{\psi}_q^r(x) (i \not{D} - m)_{rs} \psi_q^s(x) + \mathcal{L}_{gauge-fixing} + \mathcal{L}_{ghost}$$

- where
- $F_{\mu\nu}^A = \partial_\mu G_\nu^A - \partial_\nu G_\mu^A - g_s f^{ABC} G_\mu^B G_\nu^C$
- $f_{ABE} f_{ECD} + f_{CBE} f_{AED} + f_{DBE} f_{ACE} = 0$
- g_s is the strong coupling

- ▶ Properties:

- ⇒ **Confinement**
- ⇒ **Asymptotic freedom**



QCD: Basics

- ▶ Describes the strong interactions among **quarks** (ψ_q) and **gluons** (G_μ^A)
- ▶ invariant properties of the symmetry group $SU(N_c)$, $N_c = 3$

$$[\lambda^A, \lambda^B] = i f^{ABC} \lambda^C$$

- ▶ Lagrangian

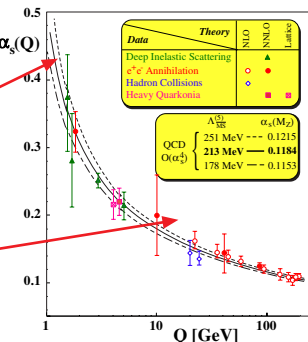
$$\mathcal{L}_{QCD} = -\frac{1}{4} F_{\mu\nu}^A(x) F_A^{\mu\nu}(x) + \sum_q \bar{\psi}_q^r(x) (i \not{D} - m)_{rs} \psi_q^s(x) + \mathcal{L}_{gauge-fixing} + \mathcal{L}_{ghost}$$

- where
- $F_{\mu\nu}^A = \partial_\mu G_\nu^A - \partial_\nu G_\mu^A - g_s f^{ABC} G_\mu^B G_\nu^C$
- $f_{ABE} f_{ECD} + f_{CBE} f_{AED} + f_{DBE} f_{ACE} = 0$
- g_s is the strong coupling

- ▶ Properties:

⇒ **Confinement**

⇒ **Asymptotic freedom**



QCD: Effective coupling

- Once it is known $\beta(\alpha_s)$

$$\frac{d\alpha_s(\tau)}{d\tau} = \beta(\alpha_s(\tau)) = Q^2 \frac{d\alpha_s(Q^2)}{dQ^2} = -b_0 \alpha_s^2(Q^2) \left(1 + \frac{b_1}{b_0} \alpha_s(Q^2) + \frac{b_2}{b_0} \alpha_s^2(Q^2) + \dots \right)$$

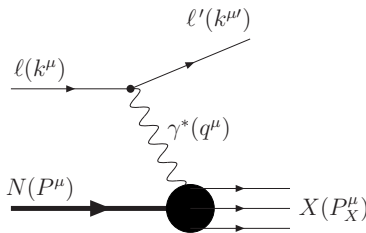
- Usually is used LO and NLO terms → expansion (only b_0 and b_1 are considered)
- ...

$$\alpha_s^{LO}(Q^2) = \frac{4\pi}{\beta_0 \ln \left(\frac{Q^2}{\Lambda^2} \right)}$$

$$\alpha_s^{NLO}(Q^2) = \frac{4\pi}{\beta_0 \ln \left(\frac{Q^2}{\Lambda^2} \right)} \left[1 - \frac{\beta_1}{\beta_0^2} \frac{\ln \ln \left(\frac{Q^2}{\Lambda^2} \right)}{\ln \left(\frac{Q^2}{\Lambda^2} \right)} \right]$$

- $\beta_0 = b_0/4\pi$ e $\beta_1 = b_1/16\pi^2$

QCD: Deep inelastic scattering



Kinematical variables

- Centre-of-mass $\gamma^* N$ energy squared

$$W^2 = (P + q)^2 \geq m_p^2$$

- Virtuality

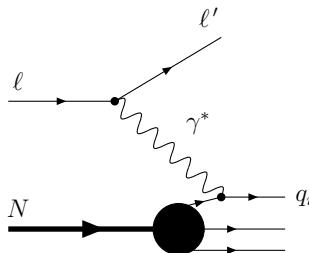
$$Q^2 \equiv -q^2 = (k - k')^2 > 0$$

- Bjorken variable, $0 \leq x \leq 1$

$$x = \frac{Q^2}{2p \cdot q} = \frac{Q^2}{Q^2 + W^2 - m_p^2}$$

- Inelasticity, $0 \leq y \leq 1$

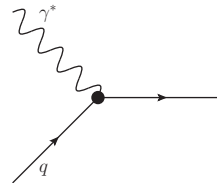
$$y = \frac{\nu}{E} = \frac{W^2 + Q^2 - m_p^2}{s - m_p^2}$$



QCD: Parton density

Parton model $\mathcal{O}(\alpha_{em})$

$$F_2 = 2x F_1 = x \sum_i e_i^2 f_i(x)$$



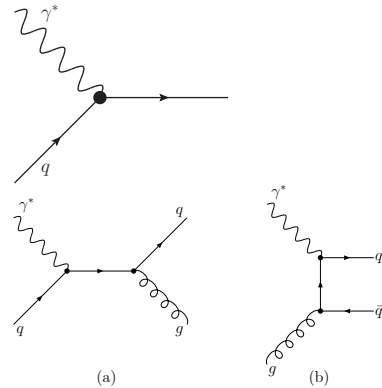
QCD: Parton density

Parton model $\mathcal{O}(\alpha_{em})$

$$F_2 = 2x F_1 = x \sum_i e_i^2 f_i(x)$$

QCD correction $\mathcal{O}(\alpha_s)$

$$F_2(x, Q^2) = \sum_{i=q, \bar{q}, g} e_i^2 x f_i(\xi, \mu^2) C^i(z, Q^2, \mu^2)$$



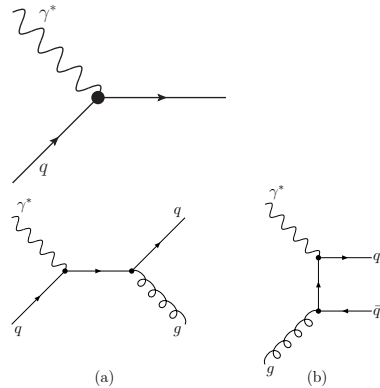
QCD: Parton density

Parton model $\mathcal{O}(\alpha_{em})$

$$F_2 = 2x F_1 = x \sum_i e_i^2 f_i(x)$$

QCD correction $\mathcal{O}(\alpha_s)$

$$F_2(x, Q^2) = \sum_{i=q, \bar{q}, g} e_i^2 x f_i(\xi, \mu^2) C^i(z, Q^2, \mu^2)$$



- ## ► DGLAP evolution

$$\frac{\partial \mathcal{U}(x, Q^2)}{\partial \ln Q^2} = \frac{\alpha_s}{2\pi} \int_x^1 \frac{d\xi}{\xi} \begin{pmatrix} P_{qq}(z, Q^2) & 2N_f P_{qg}(z, Q^2) \\ P_{gq}(z, Q^2) & P_{gg}(z, Q^2) \end{pmatrix} \begin{pmatrix} f_q(x, Q^2) \\ f_g(x, Q^2) \end{pmatrix}$$

Parton model

Distribution functions

- ▶ General hadronic collision $A + B \rightarrow C + D$

$$\sigma_{AB \rightarrow CD} = \sum_{a,b} \int_{x_a}^1 d\xi_a \int_{x_b}^1 d\xi_b \hat{\sigma}_{ab}(\xi_a p_A, \xi_b p_B) f_{a/A}(\xi_a) f_{b/B}(\xi_b)$$

- ▶ There are many dedicated collaborations which aim to determine the behavior of the distribution functions
- ▶ Here we are using the distributions:

$$\text{CTEQ6} \Rightarrow xf(x, Q_0) = A_0 x^{A_1} (1-x)^{A_2} e^{A_3 x} (1 + e^{A_4} x)^{A_5}$$

$$\text{MSTW} \Rightarrow xf_i(x, Q_0^2) = A_i x^{-\lambda_i} (1-x)^{\eta_i} (1 + \epsilon_i \sqrt{x} + \gamma_i x)$$

$$\text{CT14} \Rightarrow xf(x, Q_0) = x^{a_1} (1-x)^{a_2} P_a(x)$$

$$\text{MMHT} \Rightarrow xf(x, Q_0^2) = A(1-x)^\eta x^\delta \left(1 + \sum_{i=1}^n a_i T_i^{Ch}(y(x)) \right)$$

QIM formalism

- ▶ Describes some hadronic processes in the interplay between perturbative and nonperturbative region
- ▶ the scattering amplitude is written by means of the eikonal formalism

$$\chi(s, b) = \chi_{\text{soft}}(s, b) + \chi_{\text{SH}}(s, b)$$

⇒ $\chi(s, b) = \chi_R(s, b) + i\chi_I(s, b)$ is the (complex) eikonal function

– we assume that $\chi(s, b)$ for pp and $\bar{p}p$ scatterings are additive with respect to the soft and semi-hard (SH) parton interactions:

$$\chi_{pp}^{\bar{p}p}(s, b) = \chi^+(s, b) \pm \chi^-(s, b)$$

- ▶ increase of $\sigma_{\text{tot}}(s)$ is directly associated with parton-parton SH scatterings

QIM formalism: The revised version of DGM

- it follows from the QCD parton model that $\chi_{SH}(s, b)$ factorizes as

$$\text{Re } \chi_{SH}(s, b) = \frac{1}{2} W_{SH}(s, b) \sigma_{QCD}(s)$$

- ▶ $W_{SH}(b)$ is an overlap density for the partons at impact parameter space b :
- ▶ $\sigma_{QCD}(s)$ is the usual QCD cross section:

$$\sigma_{QCD}(s) = \sum_{ij} \frac{1}{1 + \delta_{ij}} \int_0^1 dx_1 \int_0^1 dx_2 \int_{Q_{min}^2}^{\hat{s}/2} d|\hat{t}| \frac{d\hat{\sigma}_{ij}}{d|\hat{t}|}(\hat{s}, \hat{t}) f_{i/A}(x_1, |\hat{t}|) f_{j/B}(x_2, |\hat{t}|) \Theta\left(\frac{\hat{s}}{2} - |\hat{t}|\right)$$

where $|\hat{t}| \equiv Q^2$ e $i, j = q, \bar{q}, g$

- ▶ however, the eikonal function

$$\chi^+(s, b) = \chi_{soft}^+(s, b) + \chi_{SH}^+(s, b)$$

$$\chi^-(s, b) = \chi_{soft}^-(s, b) + \chi_{SH}^-(s, b) \simeq \chi_{soft}^-(s, b)$$

DGM2015: Integral dispersion relation

- ▶ The imaginary part of $\chi_{SH}(s, b)$ can be obtained by means of the integral dispersion relation:

$$\text{Im } \chi^+(s, b) = -\frac{2s}{\pi} \mathcal{P} \int_0^\infty ds' \frac{\text{Re } \chi^+(s', b)}{s'^2 - s^2}$$

- ▶ in this way

$$\begin{aligned} \text{Im } \chi_{SH}(s, b) &= -\frac{1}{2\pi} \int_0^\infty ds' \ln \left(\frac{s' + s}{|s' - s|} \right) \left[\sigma_{QCD}(s') \frac{dW_{SH}(s', b)}{ds'} \right] \\ &\quad - \frac{1}{2\pi} \int_0^\infty ds' \ln \left(\frac{s' + s}{|s' - s|} \right) \left[W_{SH}(s', b) \frac{d\sigma_{QCD}(s')}{ds'} \right] \\ &= I_1 + I_2 \end{aligned}$$

DGM2015: Soft contribution

- ▶ The soft eikonal is needed only to describe the **lower-energy forward data**
 - ▶ the main contribution to the asymptotic behavior of the hadronic total cross section comes from the partonic SH collisions
- ⇒ It is enough to build an **instrumental parametrization** for the soft eikonal:

$$\chi_{\text{soft}}^+(s, b) = \frac{1}{2} W_{\text{soft}}^+(b; \mu_{\text{soft}}^+) \left\{ A + \frac{B}{(s/s_0)^\gamma} e^{i\pi\gamma/2} + C \left[\ln \left(\frac{s}{s_0} \right) - i \frac{\pi}{2} \right] \right\}$$

- ▶ The **odd term**, that accounts for the difference between **pp** and **$\bar{p}p$** , channels and **vanishes at high energy**

$$\chi_{\text{soft}}^-(s, b) = \frac{1}{2} W_{\text{soft}}^-(b; \mu_{\text{soft}}^-) D \frac{e^{-i\pi/4}}{\sqrt{s/s_0}}$$

DGM2015

- Are written in terms of form factors:

$$\begin{aligned} W(b) &= \int d^2 b' \rho_A(|\mathbf{b} - \mathbf{b}'|) \rho_B(b') \\ &= \frac{1}{2\pi} \int_0^\infty dk_\perp k_\perp J_0(k_\perp b) G_A(k_\perp) G_B(k_\perp) \end{aligned}$$

– $\rho(\mathbf{b})$ is the parton density

- In terms of the form factor it is simply written as:

$$\rho(b) = \frac{1}{(2\pi)^2} \int d^2 k_\perp G(k_\perp) e^{i\mathbf{k}_\perp \cdot \mathbf{b}}$$

- **Simplest hypothesis:** $W_{SH} = W_{soft}$. This prescription is not however true in QCD parton model.

DGM2015: Energy-dependent form factors

- ▶ **Most probable**: a model which quarks and gluons has distinct spatial distributions

DGM2015: Energy-dependent form factors

- ▶ **Most probable**: a model which quarks and gluons has distinct spatial distributions
- ▶ The soft overlap densities $W_{\text{soft}}^-(b)$ and $W_{\text{soft}}^+(b)$ comes from the dipole approximation to the form factors $G_A(k_\perp)$ and $G_B(k_\perp)$
- ▶ thus, using a dipole form factor

$$G_{\text{dip}}(k_\perp; \mu) = \left(\frac{\mu^2}{k_\perp^2 + \mu^2} \right)^2$$

- ▶ one gets

$$\begin{aligned} W_{\text{soft}}^\pm(b; \mu_{\text{soft}}^\pm) &= \frac{1}{2\pi} \int_0^\infty dk_\perp k_\perp J_0(k_\perp b) G_{\text{dip}}^2(k_\perp; \mu_{\text{soft}}^\pm) \\ &= \frac{(\mu_{\text{soft}}^\pm)^2}{96\pi} (\mu_{\text{soft}}^\pm b)^3 K_3(\mu_{\text{soft}}^\pm b) \end{aligned}$$

Energy-dependent form factors

- ▶ For $W_{SH}(b)$ we consider the possibility of a "broadening" of the spatial distribution of the gluons
- ⇒ our assumption suggests an increase of the average gluon radius when \sqrt{s} increases
- ⇒ can be properly implemented using two Ansätze for $W_{SH}(b)$:

$$G_{SH}^{(m)}(s, k_\perp; \nu_{SH}) = \frac{\nu_{SH}^2}{k_\perp^2 + \nu_{SH}^2} \Rightarrow W_{SH}^{(m)}(s, b; \nu_{SH}) = \frac{\nu_{SH}^2}{4\pi} (\nu_{SH} b) K_1(\nu_{SH} b)$$

$$G_{SH}^{(d)}(s, k_\perp; \nu_{SH}) = \left(\frac{\nu_{SH}^2}{k_\perp^2 + \nu_{SH}^2} \right)^2 \Rightarrow W_{SH}^{(d)}(s, b; \nu_{SH}) = \frac{\nu_{SH}^2}{96\pi} (\nu_{SH} b)^3 K_3(\nu_{SH} b)$$

- where $\nu_{SH} = \nu_1 - \nu_2 \ln(s/s_0)$

The δ -function removes the integration over ds' ; thus, the second integral can be expressed as

$$\begin{aligned} I_2(s, b) &= -\frac{1}{2\pi} \int_0^\infty ds' \ln\left(\frac{s' + s}{|s' - s|}\right) W_{\text{SH}}(s', b) \frac{d\sigma_{\text{QCD}}(s')}{ds'} \\ &= -\frac{1}{2\pi} \sum_{ij} \frac{1}{1 + \delta_{ij}} W_{\text{SH}}\left(\frac{2|\hat{t}|}{x_1 x_2}, b\right) \int_0^1 dx_1 \int_0^1 dx_2 \int_{Q_{\min}^2}^\infty d|\hat{t}| \frac{d\hat{\sigma}_{ij}}{d|\hat{t}|}(\hat{s}, \hat{t}) \\ &\quad \times f_{i/A}(x_1, |\hat{t}|) f_{j/B}(x_2, |\hat{t}|) \ln\left(\frac{\hat{s}/2 + |\hat{t}|}{\hat{s}/2 - |\hat{t}|}\right) \end{aligned}$$

The energy-dependent form factor $W_{\text{SH}}(s, b)$ can have a monopole or a dipole form, namely, $W_{\text{SH}}^{(m)}(s, b; \nu_{\text{SH}})$ or $W_{\text{SH}}^{(d)}(s, b; \nu_{\text{SH}})$ [see Eqs. (17) and (18)]. In the case of a monopole form, the first integral on the right side of (26) can be rewritten as

$$\begin{aligned} I_1^{(m)}(s, b) &= -\frac{1}{2\pi} \int_0^\infty ds' \ln\left(\frac{s' + s}{|s' - s|}\right) \sigma_{\text{QCD}}(s') \frac{dW_{\text{SH}}^{(m)}(s', b; \nu_{\text{SH}})}{ds'} \\ &= -\frac{b}{8\pi^2} \sum_{ij} \frac{1}{1 + \delta_{ij}} \int_0^\infty \frac{ds'}{s'} \ln\left(\frac{s' + s}{|s' - s|}\right) \int_0^1 dx_1 \int_0^1 dx_2 \int_{Q_{\min}^2}^\infty d|\hat{t}| \frac{d\hat{\sigma}_{ij}}{d|\hat{t}|}(\hat{s}', \hat{t}) \\ &\quad \times f_{i/A}(x_1, |\hat{t}|) f_{j/B}(x_2, |\hat{t}|) [b\nu_2 \nu_{\text{SH}}^3 K_0(\nu_{\text{SH}} b) - 2\nu_2 \nu_{\text{SH}}^2 K_1(\nu_{\text{SH}} b)] \Theta\left(\frac{\hat{s}'}{2} - |\hat{t}|\right); \end{aligned}$$

in the case of a dipole we get

$$\begin{aligned} I_1^{(d)}(s, b) &= -\frac{1}{2\pi} \int_0^\infty ds' \ln\left(\frac{s' + s}{|s' - s|}\right) \sigma_{\text{QCD}}(s') \frac{dW_{\text{SH}}^{(d)}(s', b; \nu_{\text{SH}})}{ds'} \\ &= -\frac{b^3}{192\pi^2} \sum_{ij} \frac{1}{1 + \delta_{ij}} \int_0^\infty \frac{ds'}{s'} \ln\left(\frac{s' + s}{|s' - s|}\right) \int_0^1 dx_1 \int_0^1 dx_2 \int_{Q_{\min}^2}^\infty d|\hat{t}| \frac{d\hat{\sigma}_{ij}}{d|\hat{t}|}(\hat{s}', \hat{t}) \\ &\quad \times f_{i/A}(x_1, |\hat{t}|) f_{j/B}(x_2, |\hat{t}|) [b\nu_2 \nu_{\text{SH}}^5 K_2(\nu_{\text{SH}} b) - 2\nu_2 \nu_{\text{SH}}^4 K_3(\nu_{\text{SH}} b)] \Theta\left(\frac{\hat{s}'}{2} - |\hat{t}|\right). \end{aligned}$$

DGM2015: Infrared mass scale and the role of gluons

- ▶ The gluon distribution becomes asymptotically large at $x \rightarrow 0$
- ▶ in order to obtain $\chi_{SH}(s, b)$ we select parton-parton scattering processes containing at least one gluon in the initial state:

$gg \rightarrow gg$ (gluon-gluon scattering)

$qg \rightarrow qg$ (quark-gluon scattering)

$\bar{q}g \rightarrow \bar{q}g$ (quark-gluon scattering)

$gg \rightarrow \bar{q}q$ (gluon fusion into a quark pair)

- ⇒ plagued by infrared divergences
- ⇒ have to be regularized by means of some cutoff procedure
- ▶ one natural regulator for these infrared divergences → evidence that QCD develops an effective momentum-dependent mass for the gluons
 - this *dynamical* gluon mass mechanism introduces a natural scale
- ⇒ intrinsically linked to an infrared-finite QCD effective charge $\bar{\alpha}_s(Q^2)$

Infrared mass scale and the role of gluons

- ▶ The freezing of the QCD coupling at low energies *suggests nonperturbative effects*
- ▶ a link to dynamical mass generation for gluons → were obtained by Cornwall in order to derive a gauge invariant Schwinger-Dyson equation for the gluon propagator

$$\bar{\alpha}_s = \bar{\alpha}_s(Q^2) = \frac{4\pi}{\beta_0 \ln [(Q^2 + 4M_g^2(Q^2))/\Lambda^2]}$$

$$M_g^2 = M_g^2(Q^2) = m_g^2 \left[\frac{\ln \left(\frac{Q^2 + 4m_g^2}{\Lambda^2} \right)}{\ln \left(\frac{4m_g^2}{\Lambda^2} \right)} \right]^{-12/11}$$

⇒ $m_g = 500 \pm 200$ MeV

- ▶ Perturbative regime is recovered

$$\bar{\alpha}_s(Q^2 \gg \Lambda^2) \sim \frac{4\pi}{\beta_0 \ln \left(\frac{Q^2}{\Lambda^2} \right)} = \alpha_s^{PQCD}(Q^2)$$

Infrared mass scale and the role of gluons

- ▶ Bearing in mind DGM mechanism, the parton-parton cross sections to calculate $\sigma_{QCD}(s)$ are given by

$$\frac{d\hat{\sigma}}{d\hat{t}}(gg \rightarrow gg) = \frac{9\pi\bar{\alpha}_s^2}{2\hat{s}^2} \left(3 - \frac{\hat{t}\hat{u}}{\hat{s}^2} - \frac{\hat{s}\hat{u}}{\hat{t}^2} - \frac{\hat{t}\hat{s}}{\hat{u}^2} \right)$$

$$\frac{d\hat{\sigma}}{d\hat{t}}(qg \rightarrow qg) = \frac{\pi\bar{\alpha}_s^2}{\hat{s}^2} (\hat{s}^2 + \hat{u}^2) \left(\frac{1}{\hat{t}^2} - \frac{4}{9\hat{s}\hat{u}} \right)$$

$$\frac{d\hat{\sigma}}{d\hat{t}}(gg \rightarrow \bar{q}q) = \frac{3\pi\bar{\alpha}_s^2}{8\hat{s}^2} (\hat{t}^2 + \hat{u}^2) \left(\frac{4}{9\hat{t}\hat{u}} - \frac{1}{\hat{s}^2} \right)$$

- ⇒ at large enough Q^2 these expressions reproduce their pQCD counterparts
- ▶ for gluon-gluon process: $\hat{s} + \hat{t} + \hat{u} = 4M_g^2(Q^2)$, whilst for quark-gluon and gluon fusion: $\hat{s} + \hat{t} + \hat{u} = 2M_g^2(Q^2) + 2M_q^2(Q^2)$

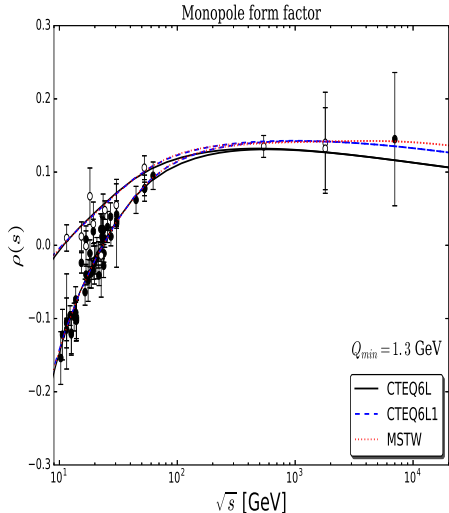
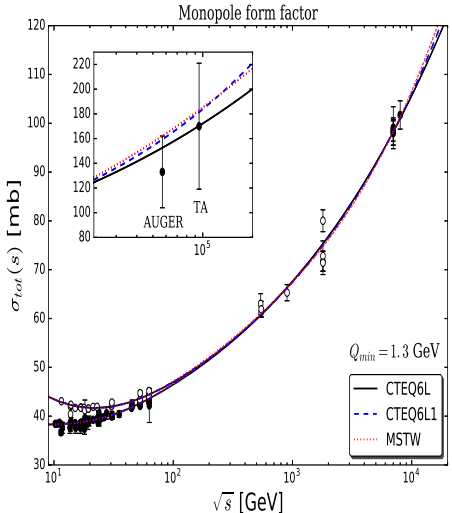
$$M_q(Q^2) = \frac{m_q^3}{Q^2 + m_q^2} \Rightarrow \text{rapidly decreases with increasing } Q$$

Results

Monopole form factor

	CTEQ6L	CTEQ6L1	MSTW
ν_1 [GeV]	1.71 ± 0.54	1.98 ± 0.75	1.52 ± 0.767
ν_2 [GeV]	0.0034 ± 0.0013	0.0052 ± 0.0016	0.00095 ± 0.00087
A [GeV $^{-2}$]	125.3 ± 14.7	107.3 ± 9.0	107.2 ± 13.6
B [GeV $^{-2}$]	43.0 ± 24.9	28.7 ± 14.7	30.5 ± 16.2
C [GeV $^{-2}$]	1.98 ± 0.68	1.22 ± 0.40	1.19 ± 0.47
γ	0.76 ± 0.19	0.70 ± 0.21	0.64 ± 0.25
μ_{soft}^+ [GeV]	0.78 ± 0.18	0.41 ± 0.27	0.48 ± 0.30
D [GeV $^{-2}$]	23.8 ± 2.0	21.4 ± 2.7	21.9 ± 2.8
μ_{soft}^- [GeV]	0.5 [fixed]	0.5 [fixed]	0.5 [fixed]
$\chi^2/154$	1.060	1.063	1.049

Results



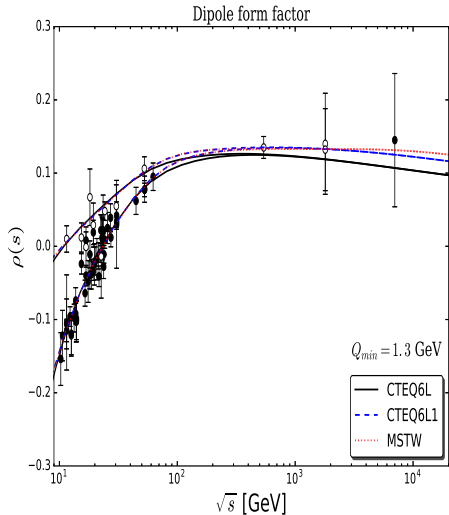
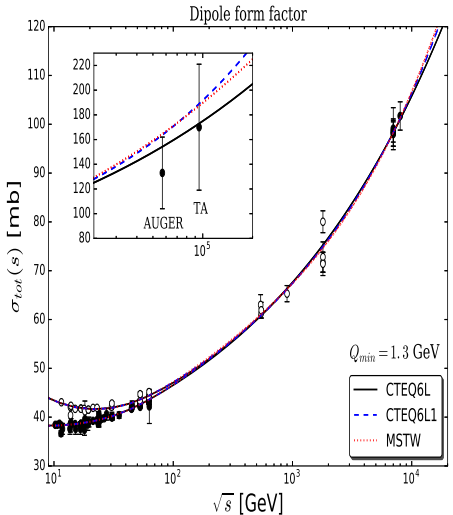
Total cross section and ρ -parameter for pp (\bullet) and $\bar{p}p$ (\circ).

Results

Dipole form factor

	CTEQ6L	CTEQ6L1	MSTW
ν_1 [GeV]	2.36 ± 0.62	2.77 ± 0.87	2.27 ± 0.85
ν_2 [GeV]	0.0051 ± 0.0042	0.0079 ± 0.0054	0.0031 ± 0.0029
A [GeV $^{-2}$]	128.9 ± 13.9	108.9 ± 8.6	108.5 ± 11.5
B [GeV $^{-2}$]	46.7 ± 26.1	30.2 ± 5.8	31.6 ± 16.2
C [GeV $^{-2}$]	2.10 ± 0.67	1.26 ± 0.44	1.23 ± 0.47
γ	0.78 ± 0.17	0.72 ± 0.20	0.66 ± 0.23
μ_{soft}^+ [GeV]	0.82 ± 0.15	0.46 ± 0.21	0.51 ± 0.24
D [GeV $^{-2}$]	24.0 ± 1.9	21.7 ± 2.3	22.1 ± 2.4
μ_{soft}^- [GeV]	0.5 [fixed]	0.5 [fixed]	0.5 [fixed]
$\chi^2/154$	1.064	1.062	1.047

Results



Total cross section and ρ -parameter for pp (\bullet) and $\bar{p}p$ (\circ).

	\sqrt{s} [TeV]	σ_{tot} [mb]		ρ	
		monopole	dipole	monopole	dipole
CTEQ6L	8.0	100.9 ^{+8.6} _{-7.3}	101.0 ^{+8.6} _{-7.3}	0.115 ^{+0.009} _{-0.008}	0.106 ^{+0.009} _{-0.007}
	13.0	111.5 ^{+9.7} _{-8.4}	111.7 ^{+9.7} _{-8.4}	0.110 ^{+0.010} _{-0.008}	
	14.0	113.2 ^{+9.9} _{-8.6}	113.5 ^{+9.9} _{-8.6}	0.110 ^{+0.010} _{-0.008}	0.100 ^{+0.009} _{-0.008}
	57.0	152.5 ^{+15.4} _{-14.7}	154.1 ^{+15.6} _{-14.9}	0.097 ^{+0.010} _{-0.010}	0.088 ^{+0.009} _{-0.009}
	95.0	170.3 ^{+17.2} _{-16.5}	172.9 ^{+17.5} _{-16.8}	0.092 ^{+0.010} _{-0.010}	0.083 ^{+0.009} _{-0.009}
CTEQ6L1	8.0	101.1 ^{+8.6} _{-7.3}	101.2 ^{+8.6} _{-7.3}	0.134 ^{+0.012} _{-0.009}	0.124 ^{+0.011} _{-0.009}
	13.0	112.4 ^{+9.8} _{-8.5}	112.9 ^{+9.8} _{-8.5}	0.131 ^{+0.012} _{-0.010}	0.120 ^{+0.011} _{-0.009}
	14.0	114.2 ^{+10.0} _{-8.7}	114.9 ^{+10.0} _{-8.7}	0.130 ^{+0.012} _{-0.010}	0.119 ^{+0.011} _{-0.009}
	57.0	159.3 ^{+16.1} _{-15.4}	163.7 ^{+16.5} _{-15.8}	0.117 ^{+0.012} _{-0.012}	0.106 ^{+0.011} _{-0.011}
	95.0	181.5 ^{+18.3} _{-17.6}	188.9 ^{+19.0} _{-18.4}	0.112 ^{+0.012} _{-0.012}	0.101 ^{+0.011} _{-0.011}
MSTW	8.0	101.3 ^{+8.6} _{-7.3}	101.3 ^{+8.7} _{-7.3}	0.142 ^{+0.013} _{-0.010}	0.131 ^{+0.012} _{-0.009}
	13.0	113.3 ^{+9.9} _{-8.5}	113.6 ^{+9.9} _{-8.5}	0.139 ^{+0.012} _{-0.011}	0.128 ^{+0.011} _{-0.010}
	14.0	115.4 ^{+10.1} _{-8.7}	115.7 ^{+10.1} _{-8.8}	0.139 ^{+0.013} _{-0.011}	0.128 ^{+0.012} _{-0.010}
	57.0	162.1 ^{+16.4} _{-15.6}	164.7 ^{+16.6} _{-15.9}	0.127 ^{+0.013} _{-0.013}	0.116 ^{+0.012} _{-0.011}
	95.0	183.0 ^{+18.5} _{-17.8}	187.3 ^{+18.9} _{-18.2}	0.123 ^{+0.013} _{-0.013}	0.112 ^{+0.012} _{-0.012}

Predictions for the forward scattering amplitudes.

	\sqrt{s} [TeV]	σ_{tot} [mb]		ρ	
		monopole	dipole	monopole	dipole
CTEQ6L	8.0	100.9 ^{+8.6} _{-7.3}	101.0 ^{+8.6} _{-7.3}	0.115 ^{+0.009} _{-0.008}	0.106 ^{+0.009} _{-0.007}
	13.0	111.5 ^{+9.7} _{-8.4}	111.7 ^{+9.7} _{-8.4}	0.110 ^{+0.010} _{-0.008}	0.101 ^{+0.009} _{-0.008}
	14.0	113.2 ^{+9.9} _{-8.6}	113.5 ^{+9.9} _{-8.6}	0.110 ^{+0.010} _{-0.008}	0.100 ^{+0.009} _{-0.008}
	57.0	152.5 ^{+15.4} _{-14.7}	154.1 ^{+15.6} _{-14.9}	0.097 ^{+0.010} _{-0.010}	0.088 ^{+0.009} _{-0.009}
	95.0	170.3 ^{+17.2} _{-16.5}	172.9 ^{+17.5} _{-16.8}	0.092 ^{+0.010} _{-0.010}	0.083 ^{+0.009} _{-0.009}
CTEQ6L1	8.0	101.1 ^{+8.6} _{-7.3}	101.2 ^{+8.6} _{-7.3}	0.134 ^{+0.012} _{-0.009}	0.124 ^{+0.011} _{-0.009}
	13.0	112.4 ^{+9.8} _{-8.5}	112.9 ^{+9.8} _{-8.5}	0.131 ^{+0.012} _{-0.010}	0.120 ^{+0.011} _{-0.009}
	14.0	114.2 ^{+10.0} _{-8.7}	114.9 ^{+10.0} _{-8.7}	0.130 ^{+0.012} _{-0.010}	0.119 ^{+0.011} _{-0.009}
	57.0	159.3 ^{+16.1} _{-15.4}	163.7 ^{+16.5} _{-15.8}	0.117 ^{+0.012} _{-0.012}	0.106 ^{+0.011} _{-0.011}
	95.0	181.5 ^{+18.3} _{-17.6}	188.9 ^{+19.0} _{-18.4}	0.112 ^{+0.012} _{-0.012}	0.101 ^{+0.011} _{-0.011}
MSTW	8.0	101.3 ^{+8.6} _{-7.3}	101.3 ^{+8.7} _{-7.3}	0.142 ^{+0.013} _{-0.010}	0.131 ^{+0.012} _{-0.009}
	13.0	113.3 ^{+9.9} _{-8.5}	113.6 ^{+9.9} _{-8.5}	0.139 ^{+0.012} _{-0.011}	0.128 ^{+0.011} _{-0.010}
	14.0	115.4 ^{+10.1} _{-8.7}	115.7 ^{+10.1} _{-8.8}	0.139 ^{+0.013} _{-0.011}	0.128 ^{+0.012} _{-0.010}
	57.0	162.1 ^{+16.4} _{-15.6}	164.7 ^{+16.6} _{-15.9}	0.127 ^{+0.013} _{-0.013}	0.116 ^{+0.012} _{-0.011}
	95.0	183.0 ^{+18.5} _{-17.8}	187.3 ^{+18.9} _{-18.2}	0.123 ^{+0.013} _{-0.013}	0.112 ^{+0.012} _{-0.012}

Predictions for the forward scattering amplitudes.

DGM2019

- ▶ Very recently: TOTEM → measurements at $\sqrt{s} = 13$ TeV
 - triggered the question of: the combined behavior of σ_{tot} and ρ at high energies is a manifestation of the Odderon?
- ▶ By means of the revised version of the DGM (with some pinpoint differences):
 - detailed analysis of σ_{tot} and ρ
 - dominant amplitude at HE → even-under-crossing contribution (**Pomeron dominance**)
- ▶ selected the “best” result of DGM2015 → dipole semihard form factor
- ▶ Updated (fine-tunned) PDF sets: MMHT, CT14
 - compared with the pré-LHC CTEQ6L
- ▶ more convenient high-energy eikonal construction

DGM2019: Derivative dispersion relation

- it follows from the QCD parton model that $\chi_{SH}(s, b)$ factorizes as

$$\operatorname{Re} \chi_{SH}(s, b) = \frac{1}{2} W_{SH}(s, b) \sigma_{QCD}(s)$$

- ▶ however, the connection of the real and imaginary part:

$$\operatorname{Im} \chi_{SH}^+(s, b) = -\tan \left[\frac{\pi}{2} \frac{d}{d \ln s} \right] \operatorname{Re} \chi_{SH}^+(s, b)$$

- which is equivalent to the change of prescription $s \rightarrow -is$
- ▶ ...

$$\operatorname{Im} \chi_{SH}(s, b) = \frac{1}{2} W_{SH}(s, b) \sigma_{QCD}(s \rightarrow -is) \simeq -\frac{\pi}{4} s W_{SH}(s, b) \frac{d\sigma_{QCD}(s)}{ds}$$

DGM2019: Soft contribution

- ▶ As before...
 - ▶ The soft eikonal is needed only to describe the **lower-energy forward data**
 - ▶ the main contribution to the asymptotic behavior of the hadronic total cross section comes from the partonic SH collisions
- ⇒ It is enough to build an **instrumental parametrization** for the soft eikonal:

$$\chi_{\text{soft}}^+(s, b) = \frac{1}{2} W_{\text{soft}}^+(b; \mu_{\text{soft}}^+) \left\{ A + \frac{B}{\sqrt{s/s_0}} e^{i\pi/4} + C \left[\ln \left(\frac{s}{s_0} \right) - i \frac{\pi}{2} \right]^2 \right\}$$

- ▶ The **odd term**, that accounts for the difference between **pp** and **$\bar{p}p$** , channels and **vanishes at high energy**

$$\chi_{\text{soft}}^-(s, b) = \frac{1}{2} W_{\text{soft}}^-(b; \mu_{\text{soft}}^-) D \frac{e^{-i\pi/4}}{\sqrt{s/s_0}}$$

DGM2019

- ▶ Notice that χ_{soft} represents the long-range Regge exchanges;
 - $\chi_{\text{soft}}^- \rightarrow$ exchange of $C = -1$ meson trajectories
 - $\chi_{\text{soft}}^+ \rightarrow$ exchange of $C = +1$ meson trajectories
- ▶ Expected: characteristic radius of the odd exchanges to be larger than the even ones
- ▶ Remember that (dipole semihard formfactor):

$$G_{SH}^{(d)}(s, k_\perp; \nu_{SH}) = \left(\frac{\nu_{SH}^2}{k_\perp^2 + \nu_{SH}^2} \right)^2 \Rightarrow W_{SH}^{(d)}(s, b; \nu_{SH}) = \frac{\nu_{SH}^2}{96\pi} (\nu_{SH} b)^3 K_3(\nu_{SH} b)$$

- where $\nu_{SH} = \nu_1 - \nu_2 \ln(s/s_0)$

DGM2019

- ▶ Notice that χ_{soft} represents the long-range Regge exchanges;
 - $\chi_{\text{soft}}^- \rightarrow$ exchange of $C = -1$ meson trajectories (ρ and ω)
 - $\chi_{\text{soft}}^+ \rightarrow$ exchange of $C = +1$ meson trajectories (a_2 and f_2)
- ▶ Expected: characteristic radius of the odd exchanges to be larger than the even ones
- ▶ Remember that (dipole semihard formfactor):

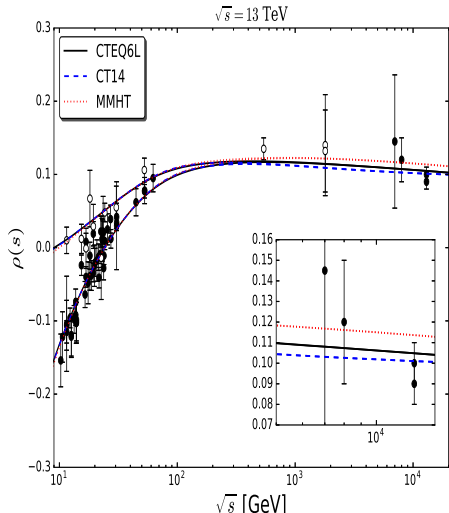
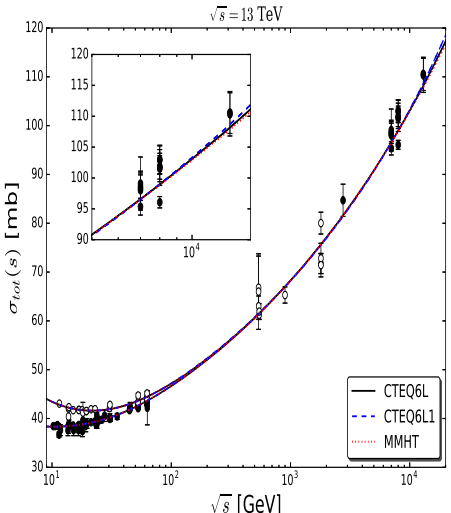
$$G_{SH}^{(d)}(s, k_\perp; \nu_{SH}) = \left(\frac{\nu_{SH}^2}{k_\perp^2 + \nu_{SH}^2} \right)^2 \Rightarrow W_{SH}^{(d)}(s, b; \nu_{SH}) = \frac{\nu_{SH}^2}{96\pi} (\nu_{SH} b)^3 K_3(\nu_{SH} b)$$

- where $\nu_{SH} = \nu_1 - \nu_2 \ln(s/s_0)$

Results: Energy cut $\sqrt{s} = 13 \text{ TeV}$

Energy	PDF:	CTEQ6L	CT14	MMHT
$\sqrt{s_{max}} = 13 \text{ (TeV)}$	$\mu_{soft}^+ [\text{GeV}]$	0.90 ± 0.20	0.90 ± 0.19	0.71 ± 0.11
	$A [\text{GeV}^{-2}]$	121.8 ± 4.6	123.5 ± 6.4	107 ± 30
	$B [\text{GeV}^{-2}]$	43.1 ± 9.0	42 ± 10	40.0 ± 6.2
	$C [\text{GeV}^{-2}]$	0.51 ± 0.21	0.67 ± 0.22	0.29 ± 0.14
	$\mu_{soft}^- [\text{GeV}]$	0.5 [fixed]	0.5 [fixed]	0.5 [fixed]
	$D [\text{GeV}^{-2}]$	24.2 ± 1.4	24.2 ± 1.5	23.3 ± 1.3
	$\nu_1 [\text{GeV}]$	2.10 ± 0.46	2.32 ± 0.52	2.11 ± 0.44
	$\nu_2 [\text{GeV}]$	0.039 ± 0.029	0.055 ± 0.034	0.030 ± 0.027
	$\chi^2/167$	1.188	1.176	1.210
	$P(\chi^2)$	4.9×10^{-2}	5.9×10^{-2}	3.3×10^{-2}

Results: Energy cut $\sqrt{s} = 13$ TeV

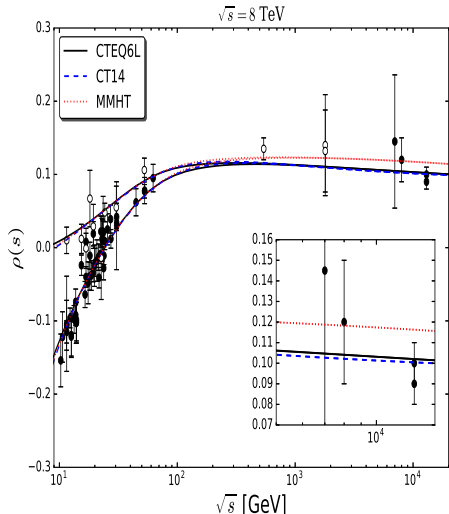
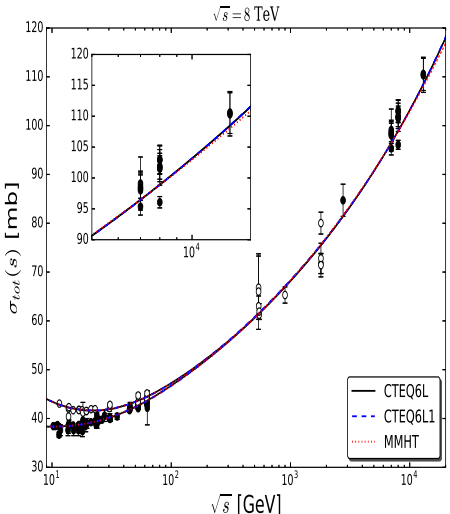


Total cross section and ρ -parameter for pp (\bullet) and $\bar{p}p$ (\circ).

Results: Energy cut $\sqrt{s} = 8$ TeV

Energy	PDF:	CTEQ6L	CT14	MMHT
$\sqrt{s_{max}} = 8$ (TeV)	$\mu_{soft}^+ [GeV]$	0.90 ± 0.20	0.90 ± 0.19	0.90 ± 0.19
	$A [GeV^{-2}]$	124.8 ± 2.4	123.6 ± 2.3	123.3 ± 2.3
	$B [GeV^{-2}]$	38.5 ± 8.1	42.1 ± 7.9	42.1 ± 7.9
	$C [GeV^{-2}]$	0.61 ± 0.14	0.73 ± 0.14	0.60 ± 0.15
	$\mu_{soft}^- [GeV]$	0.5 [fixed]	0.5 [fixed]	0.5 [fixed]
	$D [GeV^{-2}]$	24.2 ± 1.4	24.2 ± 1.4	24.2 ± 1.4
	$\nu_1 [GeV]$	2.32 ± 0.49	2.36 ± 0.54	2.04 ± 0.48
	$\nu_2 [GeV]$	0.051 ± 0.032	0.057 ± 0.035	0.027 ± 0.031
	$\chi^2/163$	1.202	1.192	1.179
	$P(\chi^2)$	4.0×10^{-2}	4.7×10^{-2}	5.8×10^{-2}

Results: Energy cut $\sqrt{s} = 8$ TeV

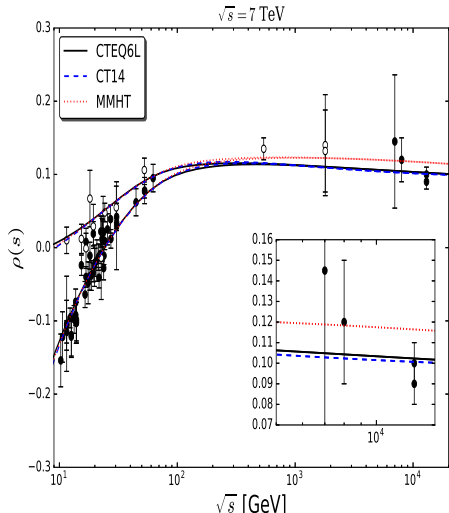
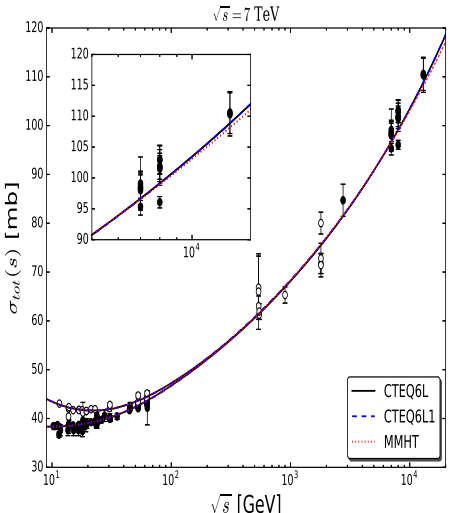


Total cross section and ρ -parameter for pp (\bullet) and $\bar{p}p$ (\circ).

Results: Energy cut $\sqrt{s} = 7$ TeV

Energy	PDF:	CTEQ6L	CT14	MMHT
$\sqrt{s_{max}} = 7$ (TeV)	$\mu_{soft}^+ [GeV]$	0.90 ± 0.20	0.90 ± 0.16	0.90 ± 0.20
	$A [GeV^{-2}]$	124.8 ± 2.4	123.6 ± 2.3	123.3 ± 2.3
	$B [GeV^{-2}]$	38.6 ± 8.2	42.2 ± 7.9	42.1 ± 8.0
	$C [GeV^{-2}]$	0.62 ± 0.14	0.73 ± 0.14	0.60 ± 0.16
	$\mu_{soft}^- [GeV]$	0.5 [fixed]	0.5 [fixed]	0.5 [fixed]
	$D [GeV^{-2}]$	24.2 ± 1.4	24.2 ± 1.4	24.2 ± 1.4
	$\nu_1 [GeV]$	2.34 ± 0.52	2.38 ± 0.60	2.05 ± 0.52
	$\nu_2 [GeV]$	0.052 ± 0.036	0.058 ± 0.041	0.029 ± 0.036
		$\chi^2/156$	1.125	1.114
		$P(\chi^2)$	1.4×10^{-1}	1.6×10^{-1}
				1.8×10^{-1}

Results: Energy cut $\sqrt{s} = 7$ TeV



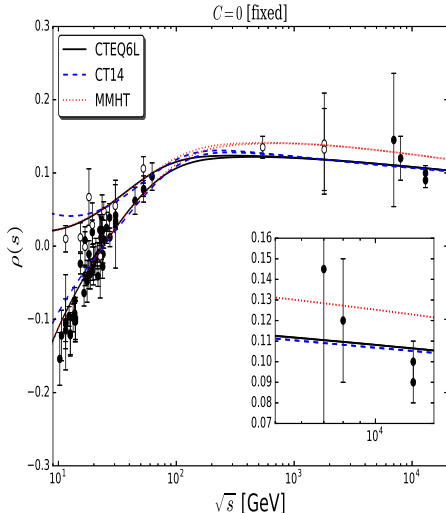
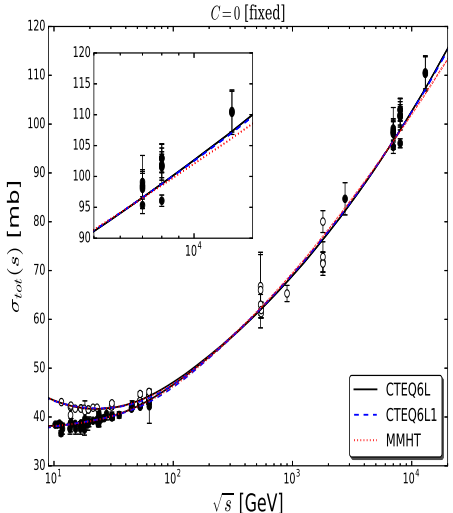
Total cross section and ρ -parameter for pp (\bullet) and $\bar{p}p$ (\circ).

Results: Effects of the leading contribution in $\chi_{soft}^+(s, b)$

$C = 0$ [fixed]

PDF:	CTEQ6L	CT14	MMHT
$\mu_{soft}^+ [\text{GeV}]$	0.700 ± 0.028	0.700 ± 0.011	0.700 ± 0.020
$A [\text{GeV}^{-2}]$	112.48 ± 0.72	118.00 ± 0.61	110.26 ± 0.80
$B [\text{GeV}^{-2}]$	24.2 ± 3.1	11.5 ± 2.8	26.9 ± 3.3
$\mu_{soft}^- [\text{GeV}]$	0.5 [fixed]	0.5 [fixed]	0.5 [fixed]
$D [\text{GeV}^{-2}]$	23.4 ± 1.3	23.6 ± 1.3	23.5 ± 1.3
$\nu_1 [\text{GeV}]$	1.82 ± 0.17	1.74 ± 0.20	1.50 ± 0.17
$\nu_2 [\text{GeV}]$	0.023 ± 0.012	0.022 ± 0.014	-0.004 ± 0.012
$\chi^2/168$	1.284	1.757	1.438
$P(\chi^2)$	7.6×10^{-3}	5.0×10^{-9}	1.7×10^{-4}

Results: Effects of the leading contribution in $\chi_{soft}^+(s, b)$



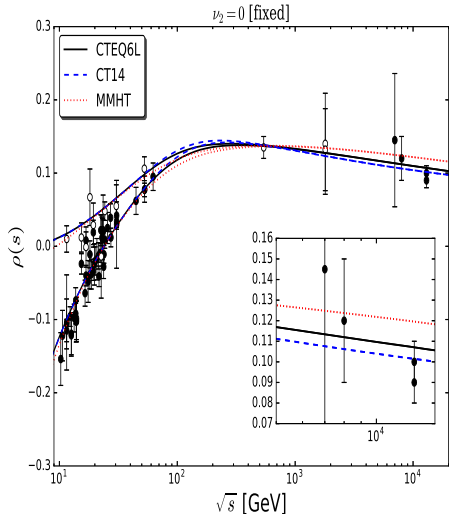
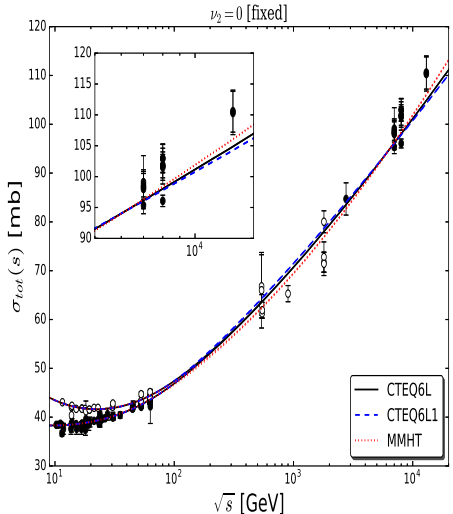
Total cross section and ρ -parameter for pp (\bullet) and $\bar{p}p$ (\circ).

Results: Effects of static semihard form factor

$\nu_2 = 0$ [fixed]

PDF:	CTEQ6L	CT14	MMHT
$\mu_{\text{soft}}^+ [\text{GeV}]$	0.90 ± 0.14	0.90 ± 0.13	0.80 ± 0.10
$A [\text{GeV}^{-2}]$	123.3 ± 1.9	125.6 ± 1.9	119.6 ± 2.4
$B [\text{GeV}^{-2}]$	38.0 ± 6.7	36.0 ± 6.7	46.5 ± 6.8
$C [\text{GeV}^{-2}]$	0.31 ± 0.10	0.490 ± 0.096	0.47 ± 0.11
$\mu_{\text{soft}}^- [\text{GeV}]$	0.5 [fixed]	0.5 [fixed]	0.5 [fixed]
$D [\text{GeV}^{-2}]$	24.3 ± 1.3	24.3 ± 1.3	24.3 ± 1.3
$\nu_1 [\text{GeV}]$	1.494 ± 0.032	1.470 ± 0.036	1.579 ± 0.036
$\chi^2/168$	1.330	1.407	1.260
$P(\chi^2)$	2.7×10^{-3}	4.0×10^{-4}	1.3×10^{-2}

Results: Effects of static semihard form factor



Total cross section and ρ -parameter for pp (\bullet) and $\bar{p}p$ (\circ).

Conclusions on DGM19

- ▶ Correct forward data set → **TOTEM + ATLAS**
- ▶ $\sqrt{s} = 13 \text{ TeV}$: plenty agreement with all the σ_{tot} data, as for ρ is quite well described only with **CTEQ6L** and **CT14**.
 - **CT14** provides exactly $\rho = 0.1$ at 13 TeV
 - conclude that our QCD-based model with **CTEQ6L** and **CT14** present simultaneous agreement with σ_{tot} and ρ at 13 TeV.
- ▶ The present scenario **doesn't change** if we exclude from the data set the experimental information at **13 TeV** ($\sqrt{s_{\text{max}}} = 8 \text{ TeV}$) and even also the data at **8 TeV** ($\sqrt{s_{\text{max}}} = 7 \text{ TeV}$)
 - powerful predictive character of **DGM19**
 - low- x parton distribution effects **was already present in pré-LHC set**
- ▶ The very good description of $\sigma^{pp, \bar{p}\bar{p}}$ and $\rho^{pp, \bar{p}\bar{p}}$ → strongly related to the energy dynamics present in the semihard form factor
 - **Pomeron dominance** present in the even soft eikonal
 - why poorly result with **MMHT**?

General conclusions and final remarks

- ▶ Elastic hadronic collision description
 - Regge theory
 - QCD inspired
- ▶ Motivated by:
 - Recent measurements of σ_{tot}^{pp} and ρ^{pp} at $\sqrt{s} = 13$ TeV
- ▶ Forward analysis: we concluded that the correct ensemble **must be constructed taking into account** the whole experimental data available, i.e. by including **TOTEM + ATLAS**
- ▶ Nonforward or nearforward analysis: the inclusion of **ATLAS** may cause some kind of bias.
- ▶ Nevertheless the unexpected decrease of $\rho^{pp}(s)$ and the expected increase of $\sigma_{tot}^{pp}(s)$
 - we were able to study the **high-energy** behavior of the elastic hadronic scattering amplitude
 - to provide quite good predictions to $\sigma_{tot}^{pp, \bar{p}p}$
 - in some cases: excellent agreement with the trend of measurements of ρ^{pp} at $\sqrt{s} = 13$ TeV
 - an in one approach to study the qualitative behavior of $\sigma_{el}^{diff, pp}$ for $t \leq 0.1$ GeV²

General conclusions and final remarks

- * **Soft Pomeron models:** we found at least one parametrization with double- and triple-pole that cannot be excluded by the bulk of experimental results (**Model III**)
 - we carried out the theoretical uncertainty propagation with both **1** and **2 standard deviations** ($\sim 68\%$ and 95% CL)
 - as far as we know, no one before have considered such error propagation analysis

$$\rho(\sqrt{s} = 13 \text{ TeV}) = 0.1185 \pm 0.0049 \text{ (ensemble T)}$$

$$\rho(\sqrt{s} = 13 \text{ TeV}) = 0.1158 \pm 0.0042 \text{ (ensemble T+A)}$$

- also for the first time, it was considered as the **most probable data set** an ensemble containing both **forward TOTEM** and **ATLAS pp** high-energy measurements
- leading **Pomeron** contributions still are in the game
- further insights on the discrepancies between the **TOTEM** and **ATLAS** data surely will be very helpful

General conclusions and final remarks

- * **Born-level and eikonal analysis:** we have explored the constraints
 - in the **Pomeron** parameters → more specifically the nonlinearity of the **Pomeron trajectory**
 - different combinations of proton-Pomeron vertices → **exponential** and a **power-like**
- ▶ **Former analysis:** beyond HE **single-Pomeron** exchange → estimated the effects of **double-Pomeron** exchange
- ▶ **As for the latter one:** the rôle of **one-** and **two-channel** construction
- ▶ **In both approaches:** the dynamical differences → mostly associated with the functional form of the vertex
 - **Eikonal analysis**, indeed, resulted in better fit curves
 - but the ρ curve didn't reach the upper error bar at $\sqrt{s} = 13 \text{ TeV}$
- ▶ There are some other possible scenarios to explore by using eikonalized amplitudes → **Perspectives**

General conclusions and final remarks

- * **Dynamical gluon mass model:** we have investigated the $p\bar{p}$ and $\bar{p}p$ scattering in the LHC energy region
 - the increase of $\sigma_{tot}^{hh} \rightarrow$ semihard interactions
 - energy-dependent semihard form factors
- ▶ **DGM2015:** integral dispersion relations specially tailored to connect the real and imaginary parts of the SH eikonal
- ▶ **DGM2019:** derivative dispersion relations \rightarrow equivalent to $s \rightarrow -is$
 - **Firstly:** pré-LHC sets: CTEQ6L, CTEQ6L1 and MSTW
 - **Secondly:** next generation sets: CT14 and MMHT, and then compared with CTEQ6L1
- ▶ **excellent results**, even if the 8 and 13 TeV data aren't included
 - low-x parton dynamics play a major rôle
- ▶ The DGM2019 provided an accurate global description of σ_{tot} and ρ with post-LHC fine-tunned PDF's such as CT14
 - amplitude dominated asymptotically by only crossing-even terms

Perspectives

* Regge-type models:

- find a way to study the theoretical error propagation in eikonalized models (very next step!)
- study the t -dependence in double- and triple Pomeron-poles → (Auberson-Martin-Kinoshita theorem)
- Consider the complete Reggeon signature form, and not the asymptotic low- t one

** QCD-based model:

- study other functional forms of energy-dependent SH form factors → associated with the σ_{el}^{diff}
- quantify the effects of Odderon-like contribution in the $\chi_{soft}^+(s, b)$ → e.g. $-\ln^2(s/s_0) + i\pi \ln(s/s_0)$

At the end of the day...

- *** *In our view our results don't contradict the recent claim that Odderon was discovered in the LHC, but strongly indicates that it is still too early for such an assertion.*

Publications in scientific journals and proceedings

1. Bahia, C.A.S., Broilo, M. and Luna, E.G.S., *Nonperturbative QCD effects in forward scattering at the LHC*, **Phys.Rev.D92** (2015) no.7 074039.
DOI: 10.1103/PhysRevD.92.074039.
2. Bahia, C.A.S., Broilo, M. and Luna, E.G.S., *Energy-dependent dipole form factor in a QCD-inspired analysis*, **J.Phys.Conf.Ser. 706** (2016) no.5 052006.
DOI: 10.1088/1742-6596/706/5/052006.
3. Bahia, C.A.S., Broilo, M. and Luna, E.G.S., *Regge phenomenology at LHC energies*, **Int.J.Mod.Phys. Conf.Ser. vol.45** (2017) 1760064.
DOI: 10.1142/S2010194517600643.
4. Broilo, M., Luna, E. G. S., and Menon, M. J., *Leading Pomeron Contributions and the TOTEM Data at 13 TeV*, **Hadron Physics 2018**.
e-Print: arXiv:1803.06560.
5. Broilo, M., Luna, E. G. S., and Menon, M. J., *Soft Pomerons and the Forward LHC Data*, **Phys.Lett. B781** (2018) 616-620.
DOI: 10.1016/j.physletb.2018.04.045.
6. Broilo, M., Luna, E. G. S., and Menon, M. J., *Forward Elastic Scattering and Pomeron Models*, **Phys.Rev.D98, 7** (2018), 074006.
DOI: 10.1103/PhysRevD.98.074006.

To be, or not to be, submitted

7. Broilo, M. and Luna, E.G.S., *The soft Pomeron and the LHC data*,
(to be submitted to Physical Review D)
8. Broilo, M. and Luna, E.G.S., *Unitarity and the simple-pole Pomeron at the LHC*,
(to be submitted to Physical Review Letter)
9. Broilo, M., Fagundes, D.A., Luna, E. G. S., and Menon, M. J.,
Proton-proton forward scattering amplitude at the LHC,
(to be submitted to Physical Review Letter)
10. Broilo, M., Fagundes, D.A., Luna, E. G. S., and Menon, M. J., *LHC13 forward elastic scattering data: Dynamical gluon mass and semi-hard interactions*,
(to be submitted to Physical Review D)

Back up

Eikonal formalism

- ▶ If, however, the profile function is written according to Durand & Pi prescription

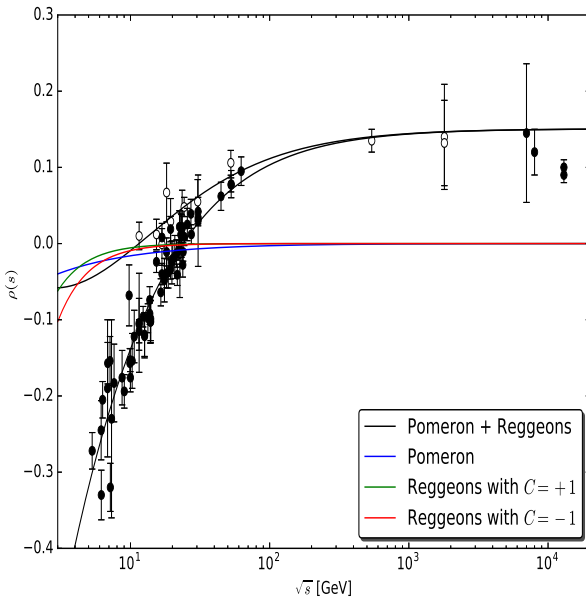
$$\Gamma(s, b) = 1 - e^{-\chi(s, b)}$$

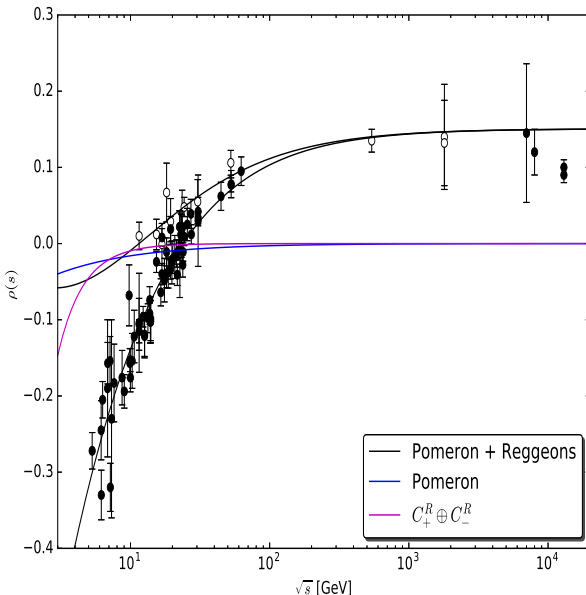
- ▶ Total cross section

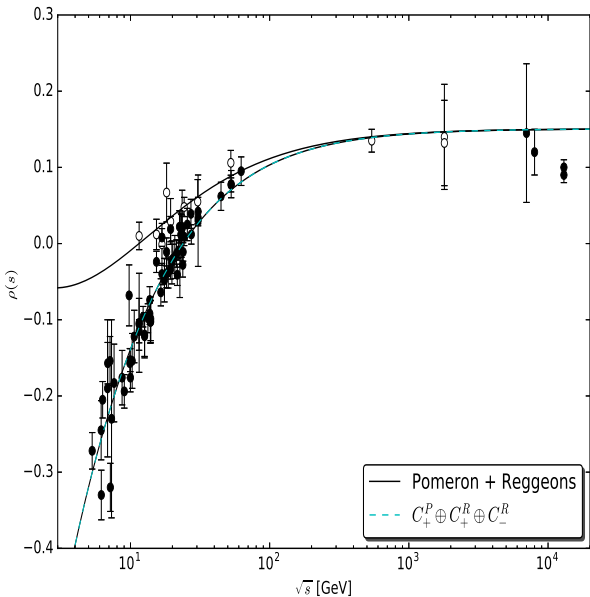
$$\sigma_{tot}(s) = 4\pi \int_0^\infty db b [1 - e^{-\chi_R} \cos \chi_I] = \sigma_{el} + \sigma_{in}$$

- ▶ ρ -parameter

$$\rho(s) = -\frac{\int_0^\infty db b e^{-\chi_R} \sin \chi_I}{\int_0^\infty db b (1 - e^{-\chi_R} \cos \chi_I)}$$







Regge theory: Convergence domain

- ▶ The continuation to complex angular momenta naturally emerges
- ▶ At first glance

$$A(s, t) = \sum_{\ell=0}^{\infty} (2\ell + 1) A_\ell(t) P_\ell(z)$$

- gives the ***t*-channel** correct scattering representation
- physical ***t*-channel** domain: $t \geq 4m^2$ and $-1 \leq z \leq 1$
- but cannot be used in the limit of **high energies** as the crossing symmetric amplitude
- ▶ The poles are in the $A_\ell(t)$, but the energy-dependence appears in the $P_\ell(z)$
- ▶ Asymptotically at $s \rightarrow \infty$ the series diverges

Regge theory: Convergence domain

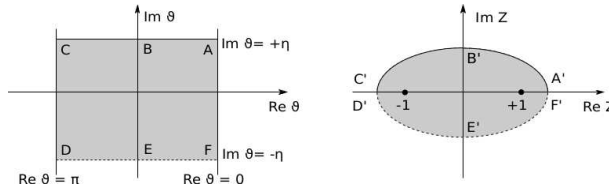
- In the case of real values of ℓ

$$\lim_{\ell \rightarrow \infty} P_\ell(\cos \vartheta) = \mathcal{O}(e^{\ell |\operatorname{Im} \vartheta|})$$

- partial wave series converges only if $A_\ell(t) e^{\ell |\operatorname{Im} \vartheta|} \leq 1$

$$\lim_{\ell \rightarrow \infty} A_\ell(t) \sim e^{-\ell \eta(t)}$$

- the convergence domain for the partial wave amplitude for $|\operatorname{Im} \vartheta| \leq \eta(t)$
- Converge in a domain **slightly larger** than the **physical one**, however **cannot** be continued to regions where s becomes arbitrarily large



Regge theory: Convergence domain

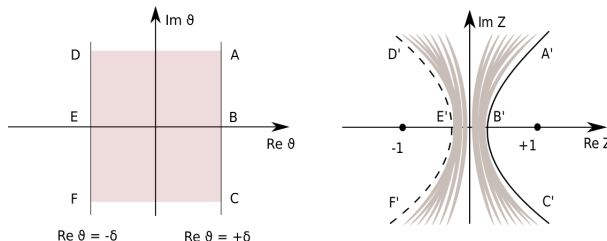
- In the case of purely imaginary values of ℓ

$$\lim_{\ell \rightarrow i\infty} P_\ell(\cos \vartheta) = O(e^{|\ell||\operatorname{Re} \vartheta|})$$

- partial wave series converges only if $A_\ell(t) e^{|\ell||\operatorname{Re} \vartheta|} \leq 1$

$$\lim_{\ell \rightarrow i\infty} A_{|\ell|}(t) \sim e^{-|\ell|\delta(t)}$$

- the convergence domain for the partial wave amplitude for $|\operatorname{Re} \vartheta| \leq \delta(t)$
- It has an ***open domain***, and therefore s can become asymptotically large



Regge theory: Regge poles

- ▶ By applying the Regge theory into **relativistic scattering**
– by means of the **Froissart-Gribov projection**:

$$A_\ell(t) = \frac{1}{\pi} \int_{z_0}^{+\infty} dz_t D_s(s(z_t, t), t) Q_\ell(z_t) + \frac{1}{\pi} \int_{-z_0}^{-\infty} dz_t D_u(u(z_t, t), t) Q_\ell(z_t)$$

- ▶ The **scattering amplitude** is written as the **Watson-Sommerfeld transform** of the **partial wave series**:

$$\begin{aligned} A(z_t, t) = & -\pi \sum_{\xi=\pm 1} \sum_{i_\xi} \frac{1 + \xi e^{-i\pi\ell}}{2} \gamma_{i_\xi}(t) (2\alpha_{i_\xi}(t) + 1) \frac{P_{\alpha_{i_\xi}}(-z_t)}{\sin \pi \alpha_{i_\xi}(t)} + \\ & + \frac{i}{2} \sum_{\xi=\pm 1} \int_{c-i\infty}^{c+i\infty} d\ell \frac{1 + \xi e^{-i\pi\ell}}{2} (2\ell + 1) A(\ell, t) \frac{P_\ell(-z_t)}{\sin \pi \ell} d\ell \end{aligned}$$

- ▶ Leading pole → **Pomeron** $\xi = +1$

$$A(s, t) \underset{s \rightarrow \infty}{\sim} -\gamma_i(t) \frac{1 + \xi e^{-i\pi\alpha(t)}}{\sin \pi \alpha(t)} s^{\alpha(t)}$$

Regge theory: Regge poles

- ▶ New quantum number, the signature $\xi = \pm 1$
 - Then $A_\ell(t)$ can be analytically continued to complex ℓ -values by means of the **Watson-Sommerfeld transform**
- ▶ The dominant contribution in the case of ***t*-channel** exchange

$$A(s, t) \underset{s \rightarrow \infty}{\simeq} \sum_{\xi=\pm 1} \sum_{i_\xi} -\gamma_{i_\xi}(t) \frac{1 + \xi e^{-i\pi\alpha_{i_\xi}(t)}}{\sin \pi\alpha_{i_\xi}(t)} s^{\alpha_{i_\xi}(t)}$$

- α_{i_ξ} defines the location of the *i*-th pole → each Reggeon contribution
- $\gamma_{i_\xi}(t)$ stands for the residue function and *phenomenologically* is related to the vertex coupling hadron-Reggeon
- ▶ **Fundamental result:**

Regge theory: Regge poles

- ▶ New quantum number, the signature $\xi = \pm 1$
 - Then $A_\ell(t)$ can be analytically continued to complex ℓ -values by means of the **Watson-Sommerfeld transform**
- ▶ The dominant contribution in the case of ***t*-channel** exchange

$$A(s, t) \underset{s \rightarrow \infty}{\simeq} \sum_{\xi=\pm 1} \sum_{i_\xi} -\gamma_{i_\xi}(t) \frac{1 + \xi e^{-i\pi\alpha_{i_\xi}(t)}}{\sin \pi\alpha_{i_\xi}(t)} s^{\alpha_{i_\xi}(t)}$$

- α_{i_ξ} defines the location of the *i*-th pole → each Reggeon contribution
- $\gamma_{i_\xi}(t)$ stands for the residue function and *phenomenologically* is related to the vertex coupling hadron-Reggeon
- ▶ **Fundamental result:** the leading complex angular momentum singularity of the partial wave amplitude **in a given channel**, determines the **asymptotic behavior** of the scattering amplitude **in the crossed channels**

Regge theory: Regge poles

- ▶ New quantum number, the signature $\xi = \pm 1$
 - Then $A_\ell(t)$ can be analytically continued to complex ℓ -values by means of the **Watson-Sommerfeld transform**
- ▶ The dominant contribution in the case of ***t*-channel** exchange

$$A(s, t) \underset{s \rightarrow \infty}{\simeq} \sum_{\xi=\pm 1} \sum_{i_\xi} -\gamma_{i_\xi}(t) \frac{1 + \xi e^{-i\pi\alpha_{i_\xi}(t)}}{\sin \pi\alpha_{i_\xi}(t)} s^{\alpha_{i_\xi}(t)}$$

- α_{i_ξ} defines the location of the *i*-th pole → each Reggeon contribution
- $\gamma_{i_\xi}(t)$ stands for the residue function and *phenomenologically* is related to the vertex coupling hadron-Reggeon

Regge pole

- ▶ **Fundamental result:** the leading complex angular momentum singularity of the partial wave amplitude **in a given channel**, determines the **asymptotic behavior** of the scattering amplitude **in the crossed channels**

Regge theory: Regge poles

Almost the whole story

- ▶ By applying the Regge theory into **relativistic scattering**
– by means of the **Froissart-Gribov projection**:

$$A_\ell(t) = \frac{1}{\pi} \int_{z_0}^{+\infty} dz_t D_s(s(z_t, t), t) Q_\ell(z_t) + \frac{1}{\pi} \int_{-z_0}^{-\infty} dz_t D_u(u(z_t, t), t) Q_\ell(z_t)$$

- ▶ The **scattering amplitude** is written as the **Watson-Sommerfeld transform** of the **partial wave series**:

$$\begin{aligned} A(z_t, t) = & - \pi \sum_{\xi=\pm 1} \sum_{i_\xi} \frac{1 + \xi e^{-i\pi\ell}}{2} \gamma_{i_\xi}(t) (2\alpha_{i_\xi}(t) + 1) \frac{P_{\alpha_{i_\xi}}(-z_t)}{\sin \pi \alpha_{i_\xi}(t)} + \\ & + \frac{i}{2} \sum_{\xi=\pm 1} \int_{c-i\infty}^{c+i\infty} d\ell \frac{1 + \xi e^{-i\pi\ell}}{2} (2\ell + 1) A(\ell, t) \frac{P_\ell(-z_t)}{\sin \pi \ell} d\ell \end{aligned}$$

- ▶ **Fundamental result:**

Regge theory: Regge poles

Almost the whole story

- ▶ By applying the Regge theory into **relativistic scattering**
– by means of the **Froissart-Gribov projection**:

$$A_\ell(t) = \frac{1}{\pi} \int_{z_0}^{+\infty} dz_t D_s(s(z_t, t), t) Q_\ell(z_t) + \frac{1}{\pi} \int_{-z_0}^{-\infty} dz_t D_u(u(z_t, t), t) Q_\ell(z_t)$$

- ▶ The **scattering amplitude** is written as the **Watson-Sommerfeld transform** of the **partial wave series**:

$$\begin{aligned} A(z_t, t) = & - \pi \sum_{\xi=\pm 1} \sum_{i_\xi} \frac{1 + \xi e^{-i\pi\ell}}{2} \gamma_{i_\xi}(t) (2\alpha_{i_\xi}(t) + 1) \frac{P_{\alpha_{i_\xi}}(-z_t)}{\sin \pi \alpha_{i_\xi}(t)} + \\ & + \frac{i}{2} \sum_{\xi=\pm 1} \int_{c-i\infty}^{c+i\infty} d\ell \frac{1 + \xi e^{-i\pi\ell}}{2} (2\ell + 1) A(\ell, t) \frac{P_\ell(-z_t)}{\sin \pi \ell} d\ell \end{aligned}$$

- ▶ **Fundamental result:** the leading complex angular momentum singularity of the partial wave amplitude **in a given channel**, determines the **asymptotic behavior** of the scattering amplitude **in the crossed channels**

Regge theory: Regge poles

Almost the whole story

- ▶ By applying the Regge theory into **relativistic scattering**
 - by means of the **Froissart-Gribov projection**:

$$A_\ell(t) = \frac{1}{\pi} \int_{z_0}^{+\infty} dz_t D_s(s(z_t, t), t) Q_\ell(z_t) + \frac{1}{\pi} \int_{-z_0}^{-\infty} dz_t D_u(u(z_t, t), t) Q_\ell(z_t)$$

- ▶ The **scattering amplitude** is written as the **Watson-Sommerfeld transform** of the **partial wave series**:

$$A(z_t, t) = -\pi \sum_{\xi=\pm 1} \sum_{i_\xi} \frac{1 + \xi e^{-i\pi\ell}}{2} \gamma_{i_\xi}(t) (2\alpha_{i_\xi}(t) + 1) \frac{P_{\alpha_{i_\xi}}(-z_t)}{\sin \pi \alpha_{i_\xi}(t)} + \\ + \frac{i}{2} \sum_{\xi=\pm 1} \int_{c-i\infty}^{c+i\infty} d\ell \frac{1 + \xi e^{-i\pi\ell}}{2} (2\ell + 1) A(\ell, t) \frac{P_\ell(-z_t)}{\sin \pi \ell} d\ell$$

Regge pole

- ▶ **Fundamental result:** the **leading complex angular momentum singularity** of the partial wave amplitude **in a given channel**, determines the **asymptotic behavior** of the scattering amplitude **in the crossed channels** →

Parameter	Value	Error
H_1 (mb)	0.24964	+0.02452 -0.03058
H_2 (mb)	-0.31854	+0.86147 -0.63729
H_3 (mb)	30.012	+4.304 -6.363
O_1 (mb)	-0.05098	+0.01050 -0.00989
O_2 (mb)	1.0240	+0.1883 -0.2097
O_3 (mb)	-4.9110	+1.0319 -0.8852
$\alpha_+(0)$	0.62957	+0.05042 -0.04803
C_+^R (mb)	47.292	+3.862 -2.879
$\alpha_-(0)$	0.26530	+0.06727 -0.07050
C_-^R (mb)	36.113	+5.177 -3.790

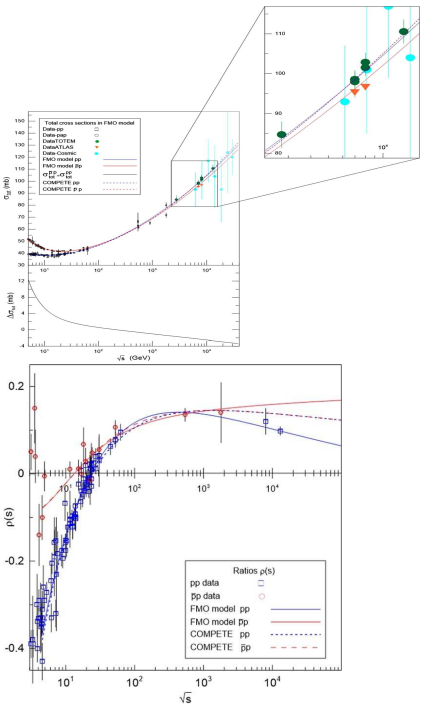
*Martynov-Nicoleescu parametrization for
 $p\bar{p}$ (black) and $\bar{p}p$ (red) processes under
the Odderon hypothesis.*

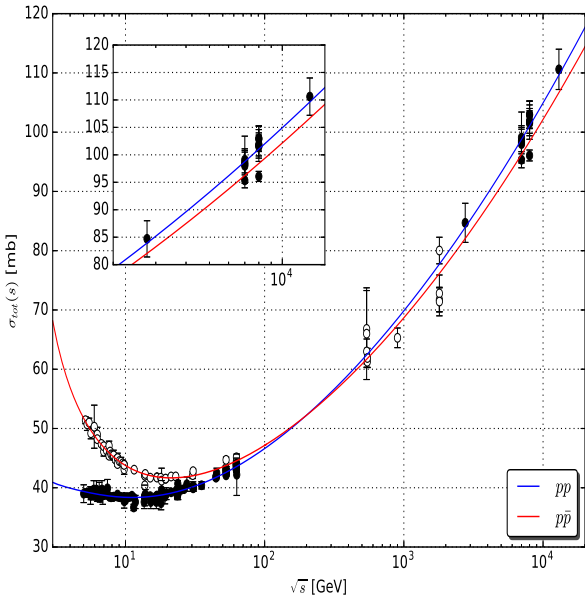
$$\chi^2/dof = 1.087$$

Parameter	Value	Error
H_1 (mb)	0.24964	+0.02452 -0.03058
H_2 (mb)	-0.31854	+0.86147 -0.63729
H_3 (mb)	30.012	+4.304 -6.363
O_1 (mb)	-0.05098	+0.01050 -0.00989
O_2 (mb)	1.0240	+0.1883 -0.2097
O_3 (mb)	-4.9110	+1.0319 -0.8852
$\alpha_+(0)$	0.62957	+0.05042 -0.04803
C_+^R (mb)	47.292	+3.862 -2.879
$\alpha_-(0)$	0.26530	+0.06727 -0.07050
C_-^R (mb)	36.113	+5.177 -3.790

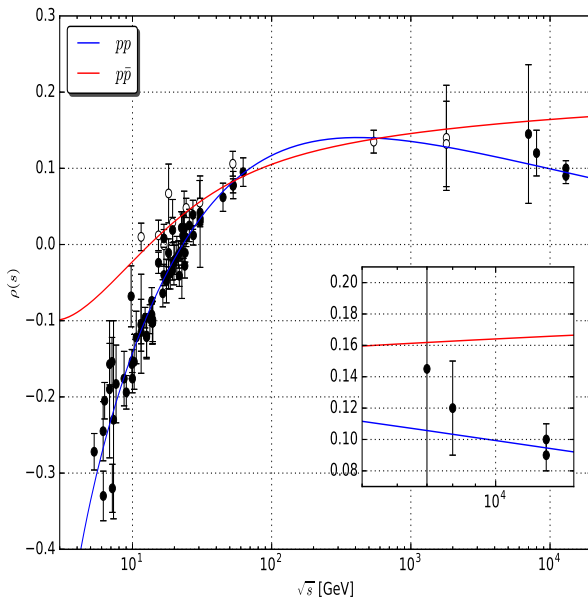
Martynov-Nicoleescu parametrization for pp (black) and $\bar{p}p$ (red) processes under the Odderon hypothesis.

$$\chi^2/dof = 1.087$$

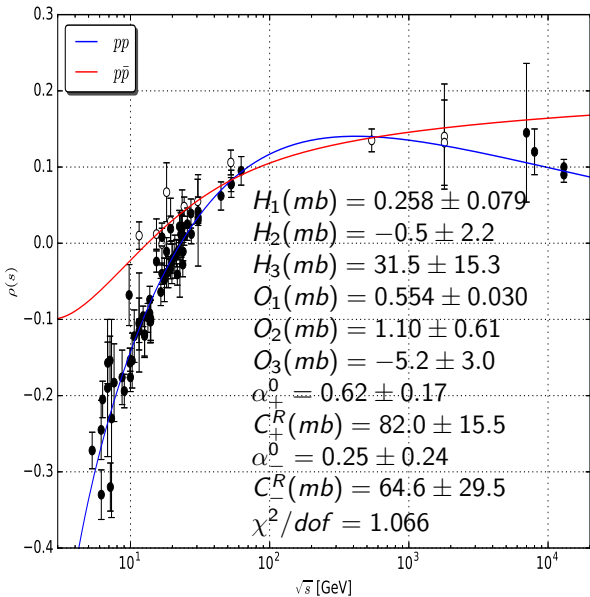




My analysis of Martynov-Nicolescu model for pp (black) and $\bar{p}p$ (red) total cross-section.



My analysis of Martynov-Nicolescu model for pp (black) and $\bar{p}p$ (red) ρ -parameter.



My analysis of Martynov-Nicolescu model for pp (black) and $\bar{p}p$ (red) ρ -parameter.

Phenomenology: Physical observables

$$(BI) \quad \sigma_{tot}^{pp, \bar{p}p} = 18.635 s^{0.0938} + 59.601 s^{-0.344} \mp 30.639 s^{-0.530}$$

$$(BII) \quad \sigma_{tot}^{pp, \bar{p}p} = 18.630 s^{0.0938} + 59.592 s^{-0.343} \mp 30.639 s^{-0.530}$$

$$(BIII) \quad \sigma_{tot}^{pp, \bar{p}p} = 18.508 s^{0.0944} + 59.364 s^{-0.341} \mp 30.606 s^{-0.530}$$

$$(BIV) \quad \sigma_{tot}^{pp, \bar{p}p} = 18.547 s^{0.0941} - 0.124 \frac{s^{1.188}}{\ln s} + 57.863 s^{-0.335} \mp 32.725 s^{-0.543}$$

QCD: Effective coupling

- ▶ Processes contributing to the appearance of **divergences**
- ▶ field rescaling → **redefinition** of physical quantities (**renormalization**)

$$g_s \rightarrow \alpha_s(\mu) = \frac{g_s^2}{4\pi}$$

- ▶ renormalization group equation:

$$\left(-\frac{\partial}{\partial \tau} + \beta(\alpha_s) \frac{\partial}{\partial \alpha_s} \right) \mathcal{R}(e^\tau, \alpha_s) = 0$$

– $\mathcal{R}(e^\tau, \alpha_s) = \mathcal{R}(1, \alpha_s(\tau)) = \alpha_s(\tau)$ is solution with boundary condition
 $\alpha_s(\tau = 0) = \alpha_s(\mu^2) = \alpha_s$

- ▶ ...
- ▶ $\tau = \int_{\alpha_s(0)}^{\alpha_s(\tau^2)} \frac{d\alpha'}{\beta(\alpha')} \quad , \quad \frac{d\alpha_s(\tau)}{d\tau} = \beta(\alpha_s(\tau)) \quad , \quad \frac{d\alpha_s(\tau)}{d\alpha_s} = \frac{\beta(\alpha_s(\tau))}{\beta(\alpha_s)}$
- ▶ scale-dependence is in α_s

QIM formalism

- ▶ In this approach the energy dependence of the $\sigma_{tot}(s)$ is obtained from the QCD using an eikonal formulation
- ▶ More specifically: behavior of the forward observables $\sigma_{tot}(s)$ and $\rho(s)$ derived from the QCD parton model
 - ⇒ standard QCD cross sections for elementary parton-parton processes
 - ⇒ updated sets of quark and gluon distribution functions
 - ⇒ physically-motivated cutoffs which restrict the parton-level processes to semi-hard (SH) ones
- ▶ SH processes arise from hard scatterings of partons carrying very small fractions of the momenta of their parent hadrons
 - ⇒ appearance of jets with $E_T \ll \sqrt{s}$

QIM formalism

- ▶ In this picture the scattering of hadrons is an incoherent summation over all possible constituent scattering
 - ⇒ increase of $\sigma_{tot}(s)$ is directly associated with parton-parton semi-hard scatterings
 - ⇒ The high-energy dependence of $\sigma_{tot}(s)$ driven mainly by processes involving the gluon contribution
- ▶ The nonperturbative character of the QCD is also manifest at the elementary level...
 - ⇒ At high energies the soft and the semi-hard components of the scattering amplitude are closely related

QIM formalism

- ▶ Task of describing $\sigma_{tot}(s)$ and $\rho(s)$ bringing up information about the infrared properties of QCD
 - ⇒ can be properly addressed by considering the possibility that the nonperturbative dynamics of QCD generate an effective gluon mass
 - ⇒ The dynamical gluon mass is intrinsically related to an infrared finite strong coupling constant
 - ⇒ its existence is strongly supported by recent QCD lattice simulations as well as by phenomenological results
- ▶ With this background in mind, our main purpose is to explore the nonperturbative dynamics of QCD in order to describe the total cross section and the ρ -parameter.

QIM formalism: The dynamical gluon mass model

- ▶ In the eikonal representation:

$$\sigma_{tot}(s) = 4\pi \int_0^\infty b \, db [1 - e^{-\chi_R(s, b)} \cos \chi_I(s, b)]$$

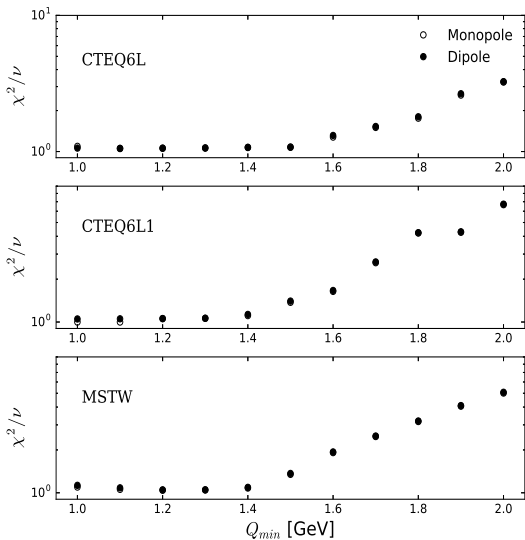
$$\sigma_{inel}(s) = \sigma_{tot}(s) - \sigma_{el}(s) = 2\pi \int_0^\infty b \, db [1 - e^{-2\chi_R(s, b)}]$$

$$\rho(s) = \frac{- \int_0^\infty b \, db e^{-\chi_R(s, b)} \sin \chi_I(s, b)}{\int_0^\infty b \, db [1 - e^{-\chi_R(s, b)} \cos \chi_I(s, b)]}$$

- $\chi(s, b) = \chi_R(s, b) + i\chi_I(s, b)$ is the (complex) eikonal function

Results so far

- ▶ We carried out a global fit to high-energy forward pp and $\bar{p}p$ scattering data above $\sqrt{s} = 10 \text{ GeV}$
- ⇒ we have included the recent data at LHC from the **TOTEM Collaboration**
- ⇒ we used a χ^2 fitting procedure as our statistical indicator, assuming an interval $\chi^2 - \chi^2_{min}$, in the case of normal errors, to the projection of the χ^2 hypersurface containing 90% of probability
- ⇒ we have investigated the effects of some updated sets of parton distributions on the high-energy cross sections, namely **CTEQ6L**, **CTEQ6L1** and **MSTW**



The χ^2/dof as a function of the cutoff Q_{min} for the monopole and the dipole semihard form factor.

Results: Partial conclusions on QIM

- ▶ The model introduces a **natural IR cutoff**
- ▶ The dynamical gluon mass M_g and the strong coupling $\bar{\alpha}_s$ are physically well motivated
- ▶ Recent lattice QCD simulations → clear evidence for the **dynamical generation of a gluon mass**
- ▶ The frozen coupling $\bar{\alpha}_s$ provides an **useful phenomenological tool** to the study of processes where a purely perturbative QCD method is inadequate
- ▶ The main contribution is that with our model we were able to study in details the $\sigma_{tot}(s)$ and $\rho(s)$.